12-2006

Dielectric Properties and Method of Characterizing Ceramic Powders and Multiphase Composites

Ravi kiran Kota
Clemson University, rkota@clemson.edu

DIELECTRIC PROPERTIES AND METHOD OF CHARACTERIZING CERAMIC POWDERS AND MULTIPHASE COMPOSITES

A Thesis
Presented to
the Graduate School of
Clemson University

In Partial Fulfillment
of the Requirements for the Degree
Master of Science
Material Science and Engineering

---

by
Ravi Kiran Kota
December 2006

Accepted by:
Dr. Burtrand. I. Lee, Committee Chair
Dr. Sarit Bhaduri
Dr. Jian Luo

ABSTRACT

Barium Titanate was the first developed ferroelectric ceramic material and it is mostly used in capacitors. The reason behind a wide range of applications is that the barium titanate boasts of high dielectric properties. A phase transition from cubic to tetragonal at normal working temperatures provides enhanced dielectric properties in this electronic material. For any application and design, the most inquired property is the dielectric constant. Knowing or predicting the dielectric constant is very much required as it forms the pre-requisite for the design of any component. This is the major objective of the present work. Driven by the nanotechnology and miniaturization of electronic devices along with volumetric efficiency, synthesis forces us to consider ever decreasing particle size of ferroelectric materials. Therefore, when we prepare or custom design nanoparticles, it is imperative to determine the electrical properties of the as-synthesized particles.

To estimate the quality of a synthesized powder relative to an already existing commercial powder, a method has been introduced to characterize the powder for dielectric constant. Chapter 1 is mainly discussed about the crystal structure, different phases, and the dielectric principles involved with barium titanate powder.

Chapter 2 is focused on the same method that has been introduced to measure the dielectric constant of polymer/ceramic composites. In this work, the dielectric constant of polyvinyl cyanoethylate/barium titanate composite was determined. The obtained results are compared with the many available theoretical models to predict the dielectric constant

of the composites. Then these results are extrapolated to comprehend the dielectric constant values of ceramic particles as these values form the base for the design of the composite.

Chapter 3 is focused on the determination of dielectric constant of a polymer/ceramic composite embedded with metallic nano-particles. The same polymer/ceramic composite that was discussed about in chapter 2 was considered with a 0.8 weight fraction of the ceramic. The precision and simplicity of the method can be exploited for predictions of the properties of nanostructure ferroelectric polymer/ceramic composites.

The characterization method developed and demonstrated in Chapters 2 & 3 is further applied for the barium titanate particle characterization. Chapter 4 is dealt with the presence of the lattice hydroxyls that is believed to be the major cause of the reduced tetragonality in the barium titanate ceramic powder. The sub-micron commercial barium titanate powder is treated with N-Methyl-2-Pyrrolidinon (NMP) to obtain a tetragonal powder. The dielectric constant of a single particle of this NMP treated cubic powder is reported to be around 64% higher than the as-received cubic powder. The dielectric properties of the barium titante ceramic powder that is determined does depend inversely on the lattice OH content as confirmed by FTIR spectroscopic analysis and TGA results.

DEDICATION

This thesis is dedicated to the memories of my late paternal grand parents Sri. Sree Rama Murthy Kota, and Smt. Seetha Ramamma Kota. I would also like to thank my maternal grand parents Late Sri. Sampoorna Kutumba Bhaskaram Kuchibhotla, and Smt. Satyavati Devi Kuchibhotla, for their blessings that helped me come out with flying colors.

ACKNOWLEDGEMENTS

First, I thank my advisor Dr. Burtrand I. Lee, for his continuous support in the Masters program. Dr. Lee was always there to listen, advice and guide me from the beginning. He taught me how to ask questions and express my ideas. He showed me different ways to approach a research problem and the need to be persistent to accomplish any goal. He is the person who is most responsible for helping me complete the writing of this thesis as well as the challenging research that lies behind it. He has been a friend and mentor. He taught me how to write academic papers and brought out the good ideas in me. Without his encouragement and constant guidance, I could not have finished this thesis. He was always there to meet and talk about my ideas, to proofread and mark up my papers and chapters, and to ask me good questions to help me think through my problems (whether philosophical or analytical). Thanks, Dr. Lee! I hope our relation flourishes and you would be as helpful as you were, all through my professional career.

Besides my advisor, I would like to thank the rest of my thesis committee: Dr. Sarit Bhaduri and Dr. Jian Luo for their friendship, encouragement, good questions, insightful comments and reviewed my work on a very short notice. During the course of this work, at Clemson University (Spring 2005 – Fall 2006), I was supported in part by Teaching Assistanship and Research Assistantship. Thanks to Dr. Kathleen Richardson, Director, School of Material Science & Engineering. Let me also say 'thank you' to the following people though they are elsewhere. Dr. Jin Hwang and Dr. Ashraf Ali, whose stay here as Post-Doctorates, greatly helped me in my thesis take-off. Thanks to Kim Ivey, for always being there and helping me with the thermal characterization techniques.

Kim, you are great! I am also greatly indebted to many teachers in the past: Mr. Sailesh Kumar for getting me interested in basic mathematics and science concepts. Thanks to Dr. Viplava Kumar, for introducing me to Metallurgy & Material Technology and teaching me all the intricacies of the subject and related skills. Dr. Ajit James and Dr. Narayana Murty deserve a special mention. After hearing my complaints and frustration with the ability of the state of material science, they helped me develop my idea and vision of what materials can do for scientists & engineers.

I appreciate my group members Gopi, Venkat, Prem, Radhika, Sujaree and Hiroki, for their words and suggestions that boosted my courage and determination to finish my research work and write this thesis. I extend my thanks to my friends, Sunil & Sunil, Kaushik, Vinod, Kiran, Anand, Ajay, Abhilash, Ram, Jeetu, and above all Gopi here in United States, Satish in Europe and Anil, Prabhakar, Ravi, Suresh and Chandu, back in India. This thesis would be incomplete without a mention of the support given me by my beloved friend, Aparna, who accompanied me in each and every aspect of my life.

Last, but not least, I thank my family: my parents, Venkata Ramana Kota and Sita Rama Lakshmi Kota, for giving me life in the first place, for educating me with aspects from both arts and sciences, for unconditional support and encouragement to pursue my interests and for reminding me that my research should always be useful and serve good purposes, my brother, Naveen Kota, for believing in me.

TABLE OF CONTENTS

Table of Contents (Continued)

LIST OF TABLES

LIST OF FIGURES

List of Figures (Continued)

PREFACE

Our goal of this project was to characterize ceramic powders and composites which are used as embedded capacitors. This work was systematically divided into three parts. The first part deals with the characterization of two-phase barium titanate/cyanoethyl ester of polyvinyl alcohol (polymer/ceramic) composite in comparison with the existing theoretical models by developing a different method of determining the dielectric constant. Commercial barium titanate and the polymer obtained from Russia were used as raw materials. The second part of the project deals with the incorporation of silver conducting particles into the polymer/ceramic matrix, using the principle of percolation. The last part of the thesis deals with phase transition and the related OH group effect on the dielectric properties of barium titanate.

Chapter 1

Introduction

Barium titanate has a typical perovskite structure which is shown in Fig.1. Perovskite materials, with general stoichiometry as ABO_3, represent a unique class of crystalline solids that demonstrate a variety of interesting dielectric, piezoelectric, ferroelectric, and electro-optic properties. The unique properties of perovskite materials are the result of the crystal structure, phase transitions as a function of temperature, and the size of the ions present in the unit cell.

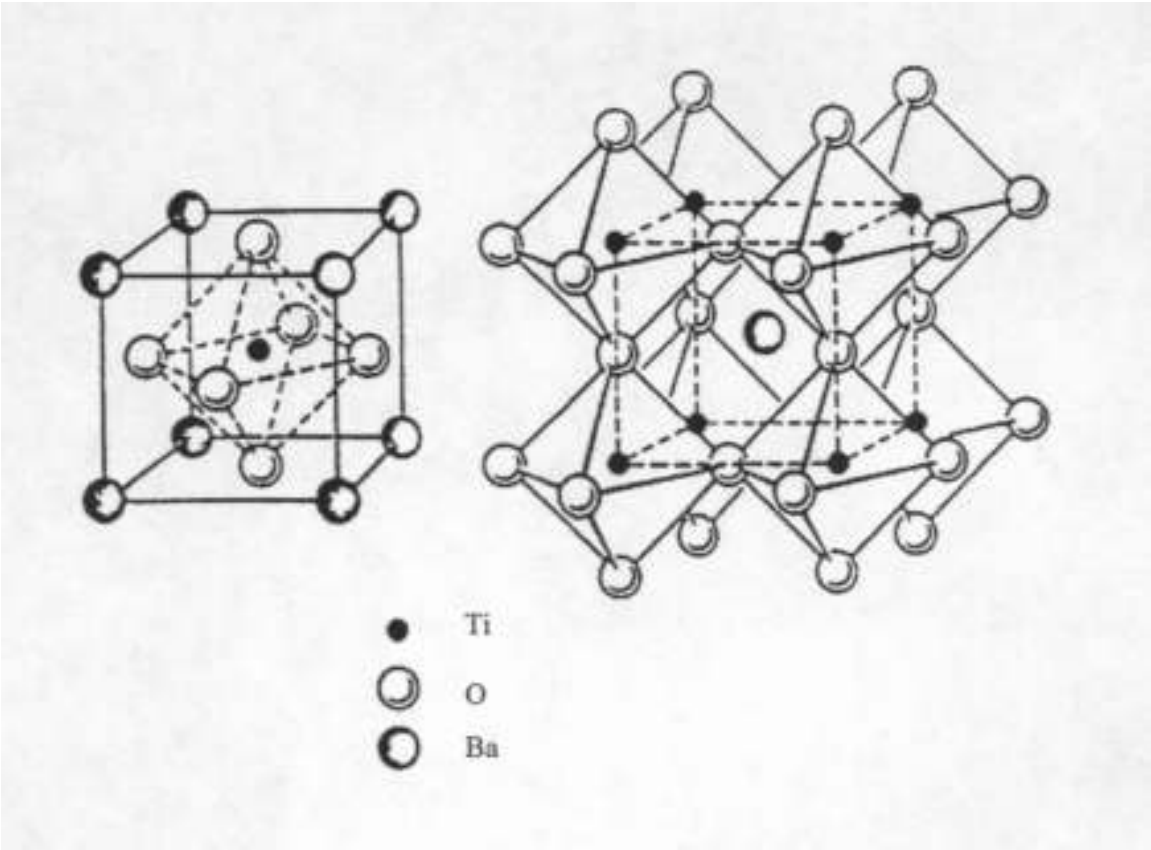

Fig. 1. Perovskite structure of $BaTiO_3$.

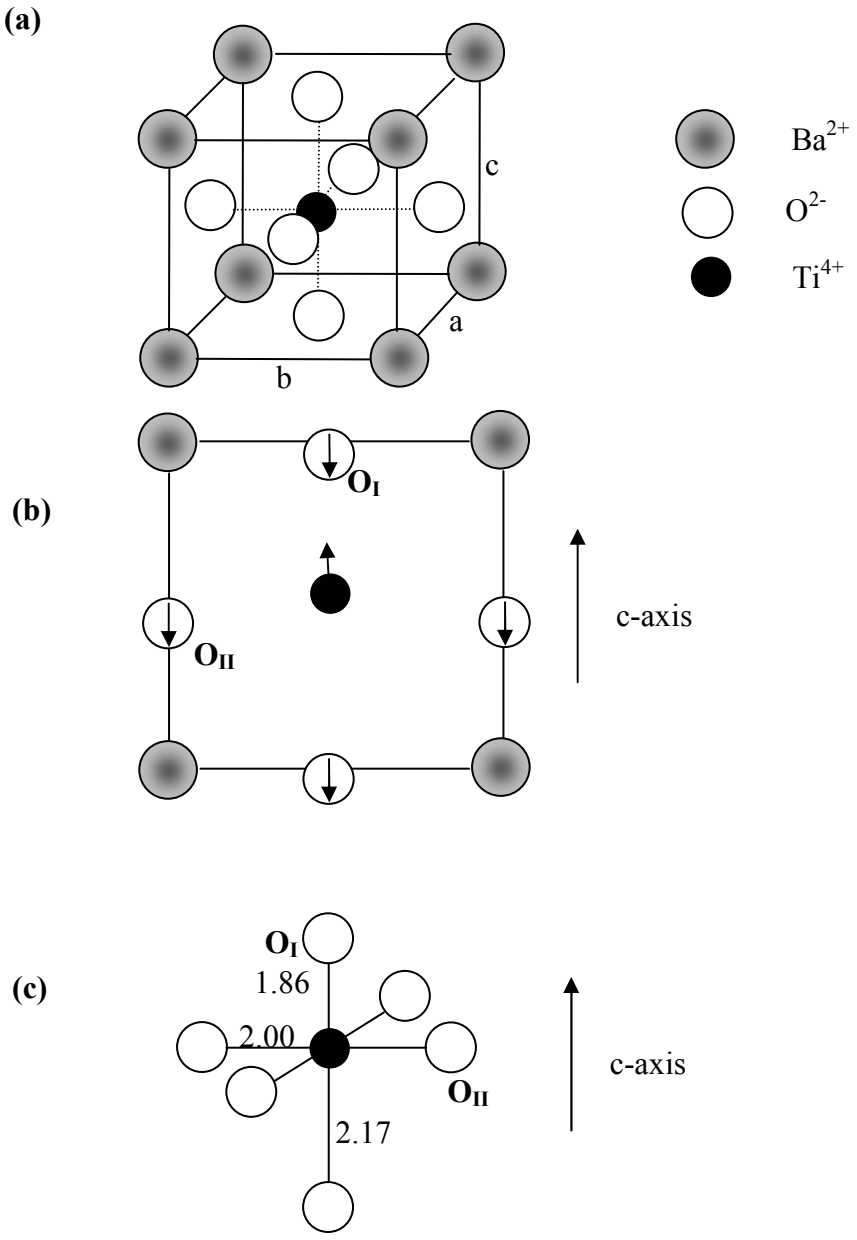

Fig. 2. (a) Perovskite structure of $BaTiO_3$ above Curie point, (b) a-axis projection of tetragonal $BaTiO_3$ with atomic displacements, and (c) $[TiO_6]$ octahedron in tetragonal phase showing displacement of Ti along c-axis.

The barium ions reside at the corners of the cubic forming a close-packed structure along with the oxygen ions, which occupy the face center of the cubic. Each barium ion is surrounded by twelve oxygen ions and each oxygen ion is surrounded by four barium ions and eight oxygen ions. In the center of the face-centered cubic unit cell, the small highly charged titanium (Ti^{4+}) ion is octahedrally coordinated by six oxygen ions.

The lattice parameter of $BaTiO_3$ is slightly larger than that of the ideal perovskite due to the size of barium ions. Because of the large size of the barium ions, the octahedral interstitial position in $BaTiO_3$ is quite large compared to the size of the titanium ions. To some extent, the titanium ions are too small to be stable in these octahedral positions and tend to position themselves in an off-centered position resulting in an electric dipole. Since each titanium ion has a + 4 charge, the degree of the polarization is very high. When an electric field is applied, titanium ions can shift from random positions to aligned positions and result in high bulk polarization and a high dielectric constant.

The crystal structure and dielectric characteristics of $BaTiO_3$ strongly depend on temperatures. Above the Curie point, 130 °C, the unit cell of $BaTiO_3$ is cubic as shown in Fig. 3. When the temperature is below the Curie temperature (130^oC), the cubic structure is slightly distorted to a ferroelectric tetragonal structure having a dipole moment along the c direction. When the temperature goes down below 5^oC, the tetragonal structure will transform to an orthorhombic ferroelectric phase with the polar axis parallel to a face diagonal. When the temperature goes down further to -90 ^oC, it will transform to a rhombohedral structure with the polar axis along a body diagonal.

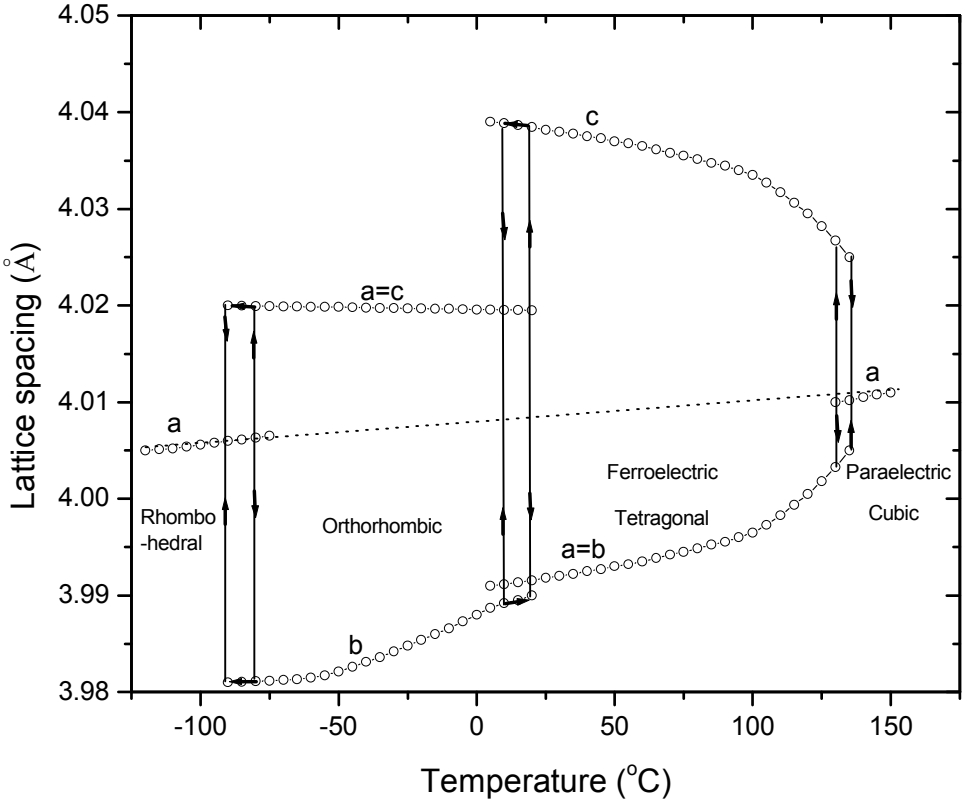

Fig. 3. Lattice parameters of single crystal $BaTiO_3$ as a function of temperature

In the temperature range of 5° to 130°C, the crystal is spontaneously polarized along a <100> direction, accompanied with tetragonal symmetry. In the range of –90° and 5°C, the crystal symmetry is orthorhombic and the direction of spontaneous polarization transfers to a pseudocubic <110>, a face diagonal of the former cubic cell. Around –90°C, a further transition to rhombohedral symmetry spontaneously polarized along a body diagonal takes place. These three transitions exhibit different electrical properties near the transition temperatures.

It results in a large change of the Ti-O bond length compared to a small change in the Ba-O bond during the cubic to tetragonal phase change. A perovskite lattice structure, the displacement of the Ti^{4+} and O^{2-} ions and the slight distortion of oxygen octahedra during the cubic to tetragonal phase transition are shown in Fig. 2. These ionic displacements also result in a change in lattice dimensions, and a negative linear thermal expansion coefficient along the c-axis, while a thermal expansion coefficient is usually positive due to a-, b-axes expansion. As shown in Fig. 3, the crystal structure of $BaTiO_3$ becomes less and less tetragonal as the temperature increases toward the tetragonal to cubic transition temperature.

Size effects in nanostructured materials are of great importance from both fundamental considerations and practical applications. The properties and behavior of macroscopic ferroelectric systems are, in principle, well known. An area, which is poorly understood at best, is so-called size effect. Initial research on size effects in ferroelectrics has concentrated on $BaTiO_3$, with the desire to understand the governing mechanisms that control the performance of multilayer capacitors as a function of layer thickness.

However, in ferroelectric fine particles, it was known that ferroelectricity decreases with decreasing particle and grain sizes, and disappears below a certain critical size. The preferred tetragonal phase of $BaTiO_3$ may be unstable at room temperature for a crystallite size below a certain size and then the stable phase is cubic. Therefore, the size effect in ferroelectrics such as $BaTiO_3$ can be considered to be one of the most important phenomena for an interest to the industry as well as to the scientific community.

$BaTiO_3$ must be modified to shift its Curie point to lower temperatures and improve the temperature coefficient of capacitance for use in capacitor devices. During

the past few decades, extensive work has been conducted to modify the dielectric properties of $BaTiO_3$ for capacitor applications by introducing different additives. In general, there are three ways to alter the structure and modify the properties of $BaTiO_3$: substitute smaller divalent ions for barium, substitute larger tetravalent ions for titanium and nonisovalent donor or acceptor doping, which is used to modify phase structure and the subsequent electrical behavior of $BaTiO_3$ dielectrics.

Dielectric properties of $BaTiO_3$

Cubic $BaTiO_3$ has paraelectric properties which show no displacement of ions, and hence, results in low dielectric permittivity. On the other hand, tetragonal $BaTiO_3$ shows ferroelectric properties which are more interesting properties of $BaTiO_3$ for dielectric applications. The temperature dependence of the relative permittivity of $BaTiO_3$ measured in a and c directions is shown in Fig. 4.

An explanation for why the dielectric constant along the c-axis is less than that along the a-axis is that oxygen ions in the c-axis, which is also cell polar axis, make strong ionic attractions with the central Ti^{4+} ion. This gives an interaction force between the Ti^{4+} and O^{2-} ions which makes vibration difficult because of a “pinning” effect under an external AC source. On the other hand, oxygen ions in the a- and b-axes are relatively free to vibrate perpendicularly to this c-axis, consequently, the dielectric constants along a- and b-axes are higher.

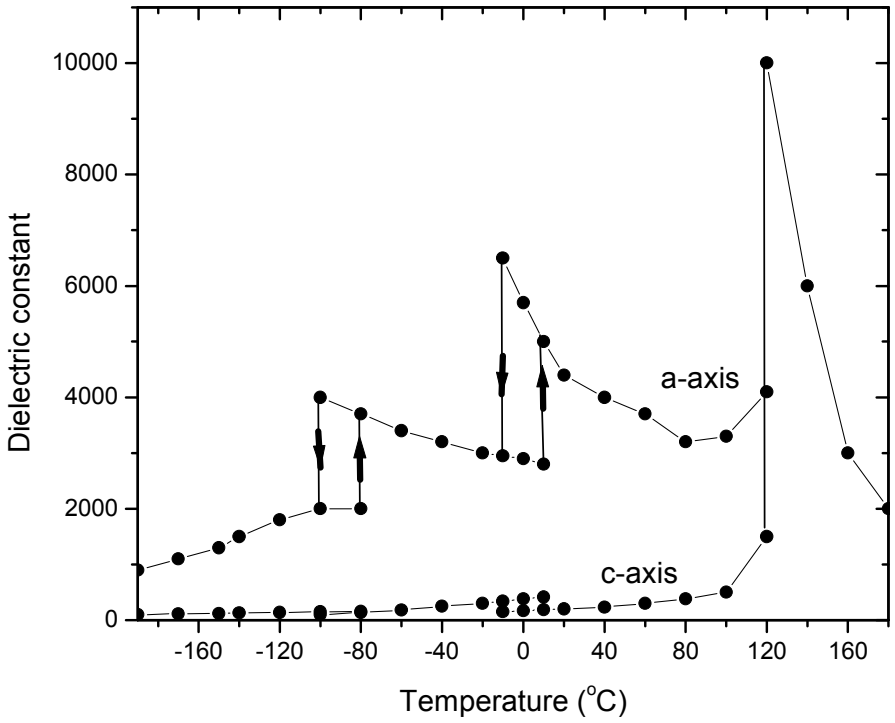

Fig. 4. Temperature and relative dielectric constant ε_a and ε_c for single crystal $BaTiO_3$

In the vicinity of the Curie point, the stability of the lattice decreases, and the amplitude of the vibration becomes higher. This induces a high dielectric constant at the Curie point. Based on these dielectric properties of a single crystal, we can infer the dielectric behavior of the polycrystalline sample or powder which is the starting material for MLCC fabrication. Although the basic dielectric properties are well known, it is worthwhile to note that the physical parameters related to the phase transition are affected by chemical purity, surface defects, particle size and sintering conditions.

Among these factors, understanding the relationship between particle size and tetragonality is especially important. This is because a recent preference for producing thinner dielectric layers and lowering sintering temperatures is dependent on fine particle

size. Generally, the belief is that there is a decrease in tetragonality, which is the c/a ratio, with decreasing particle size. This critical size difference may come from the different residual elastic strain energy, chemical impurity level and crystalline defects. Moreover, the tetragonal to cubic change is a gradual transition, and there is no clear one size factor dividing the phase completely.

Principles of Dielectrics

Dielectrics and insulators can be defined as materials with high electrical resistivities. A good dielectric is, of course, necessarily a good insulator, but the converse is by no means true. Dielectric properties, dielectric constant, dielectric loss factor, and dielectric strength will be interpreted as follow.

Capacitance

The principal characteristic of a capacitor is that an electrical charge Q can be stored. The charge on a capacitor is given in equation 1.

$$Q=CV \quad (1)$$

where V is the applied voltage and C is the capacitance. The capacitance C contains both a geometrical and a material factor. For a large plate capacitor of area A and thickness d the geometrical capacitance in vacuum is given by equation 2.

$$C_0=(A/d)*\varepsilon_0 \quad (2)$$

where ε_0 is the permittivity (dielectric constant) of a vacuum. If a ceramic material of permittivity ε' is inserted between the capacitor plates,

$$C=C_0*(\varepsilon'/\varepsilon_0)=C_0K \quad (3)$$

where K is the relative permittivity or relative dielectric constant, then the capacitance can be shown in equation 3. This is the material property that determines the capacitance of a circuit element.

Dielectric loss factor

The loss factor ε″, as shown in equation 4, is the primary criterion for the usefulness of a dielectric as an insulator material.

$$\varepsilon'' = \tan\delta/\varepsilon' \quad (4)$$

In equation 4, ε′ is dielectric constant defined above, while tanδ is the dissipation factor. For this purpose it is desirable to have a high dielectric constant and particularly a very small loss angle. Applications that are desirable to obtain a high capacitor in the smallest physical space, the high dielectric constant materials must be used and it is equally important to have a low value for the dissipation factor, tanδ.

Dielectric strength

Dielectric strength is defined when the electric field is just sufficient to initiate breakdown of the dielectric. It depends markedly on material homogeneity, specimen geometry, electrode shape and disposition, stress mode (DC, AC or pulsed) and ambient conditions.

Chapter 2

Dielectric Properties of Barium Titanate/Cyanoethyl Ester of Polyvinyl Alcohol Composites in Comparison with the Existing Theoretical Models

Abstract

A unique method has been introduced to measure the dielectric constant of polymer/ceramic composites using an effective medium instead of using the general methods of preparing bulk sintered pellets or films. In this work, a new and a simple method has been applied to measure the dielectric constant of polyvinyl cyanoethylate/barium titanate composite. The results are obtained by dispersing the ceramic powders in the polymer of a relatively low dielectric constant value. The dielectric constant of the composite is measured with varying ceramic volume percentages. The obtained results are compared with the many available theoretical models that are generally in practice to predict the dielectric constant of the composites. Then these results are extrapolated to comprehend the dielectric constant values of ceramic particles as these values form the base for the design of the composite. The precision and simplicity of the method can be exploited for predictions of the properties of nanostructure ferroelectric polymer/ceramic composites.

Introduction

Passive components in an electronic system are those electrical elements which support the active components and are characterized as resistors, inductors, and capacitors. Discrete passives are considered to be the major barrier of the miniaturization of electronic system. Assimilation of passives provides the components with the advantages like better electrical performance, higher reliability, lower cost, and improved design options [1].

Currently, interest in passive components is increasing for miniaturization and better electrical performance of electronic packages. Among various kinds of passives, focus is on decoupling capacitors, which are used for simultaneous switching noise suppression [2]. The science of embedded capacitor is a sophisticated technology with the congregation of both performance and functionality requirements for future electronic devices. One of the major hindrances for implementing this technology is the lack of dielectric materials with promising dielectric properties.

Polymer based composite is considered as a solution to the problem mentioned hitherto. Developing a composite with compatible high dielectric constant material is the major challenge of the integral capacitor technology. Polymer/ceramic composites can be used in forming capacitors because they combine the process ability of polymers and high dielectric constant of ceramics. One of the promising embedded capacitor materials is a polymer/ceramic composite which is a ceramic particle-filled polymer. It is a material utilizing both high dielectric constant of ceramic powders and good process ability of polymers. Particularly epoxy/ceramic composites have been investigated and studied due to their compatibility with printed writing boards (PWB) [3-9].

It is very important for composite material design to precisely understand the dielectric constant of ceramic particles. Many methods and models, with several quantitative rules, have been developed to predict the dielectric constant of heterogeneous two component composites counting on the basis of dielectric properties of each component, i.e., both ceramic and polymer [10-13]. However, while different models have been developed, usually little or no experimental evidence was provided to support the derived equations. So ambiguity still prevails in which model is more useful for the prediction of the effective dielectric constant of the composites.

Polymers filled with ceramics have been studied for use as dielectric materials in thick film capacitors [14]. Ceramic particle size influences the effective dielectric constant of composite dramatically. Precise prediction of the effective dielectric constant of polymer/ceramic nanocomposites forms the focal point for the design of composite materials. Many theoretical models have been proposed in the literature for simulating the electrical properties of the composites. Mostly, composite dielectrics are statistical mixtures of several components.

The models mentioned are empirical models to describe the polymer/ceramic nanocomposite property. Other efforts also have been made to predict the dielectric properties of composite using percolation theory [15–18]. The major interest in the physics of disordered materials lies in relating the macroscopic property of interest like permittivity, conductivity, etc. The effective-medium theory (EMT) is also used to set up a numerical model that can precisely predict the dielectric constant of polymer/ceramic nanocomposite [22]. The major factors that affect the dielectric properties of barium titanate ceramics are the grain size, phase contents and the types of dopants used [19-21].

Thus the dielectric property of composite can be treated in terms of an effective medium whose dielectric permittivity can be obtained by a suitable averaging over the dielectric permittivity of the two constituents [25].

For polymer/ceramic composites, the perovskite-type barium titanate is in the powder form instead of the sintered form. The removal of grain boundaries, elimination of constrained forces from neighboring grains and a drop in domain density due to decrease in the particle size will reduce the dielectric constant of BT powders [23,24]. Hence, sintered and unsintered powders of BT show a different dielectric behavior.

Our work deals with a composite medium composed of dispersed unsintered ceramic within the polymer with the sole intention of minimizing voids or pores. Though this is a relative way of characterizing the composite for dielectric constant values, the method seemed interesting and reliable for measuring the dielectric constant values of the composites and these results are hence used to extrapolate linearly only to achieve the dielectric constant value of the unsintered ceramic powder.

Materials & Procedure

The polymer/ceramic composites are prepared using the commercial ceramic powder, Cabot BT-8 (BT), (hydrothermal powder with a mean particle size of 0.2μm obtained from Cabot Performance Materials, Boyertown, PA), a cyanoethyl ester of polyvinyl alcohol (CEPVA) kindly provided by Plastpolymer J.S.Company via St. Petersburg State Institute of Technology, Russia, Castor oil, Eur. Pharm. grade, having a density of 0.957 g/cc obtained from Acros Organics and BYK-W 9010 from BYK-Chemie which is a dispersant used for a better dissolution of the ceramic powder. N,N - dimethyl formamide

(DMF) from Fisher and 2-methoxyethanol from Aldrich were used as the solvents without any prior treatment and further purification.

DMF and 2-methoxyethanol were mixed in a 1:1 volume ratio and the solid polymer was dissolved maintaining the temperature at around 65° C. The amount of solid polymer added was adjusted to get a final polymer concentration of 30% by weight. After dissolution, the solution was cooled to room temperature and magnetic stirring was continued for 12 hr in a teflon jar to obtain a clear transparent pale yellow solution. The solution was stable over a period of several weeks and did not show any signs of turbidity. In a different teflon jar, a 50% by weight suspension of the commercial ceramic powder was prepared by agitation by magnetic stirring in a similar mixed solvent of 1:1 DMF and 2-methoxyethanol.

Initially, castor oil and the BT ceramic powder were mixed in different proportions. These mixtures had a variable ceramic content of 10-50% by volume on the dry basis. Next, different amounts of both polymer solution and the BT suspensions were mixed and taken into different small containers and the mixtures were adjusted to contain the final polymer/ceramic weight ratios shown in Table 1.

Table 1. Different sample mixtures used in this study

Composite	**Ceramic wt%**	**Ceramic vol%**	**Polymer wt%**
A	70	29	30
B	75	34	25
C	80	41	20
D	85	49	15

The prepared mixtures were then gently dried at 80°-90° C under both continuous magnetic stirring and mildly reduced pressure to get rid of the solvents where viscous slurries/pastes were obtained. The dried composites were then kept under reduced pressure and used for further characterization.

The capacitor is fabricated using the same procedure that was followed in our earlier work [26] and is characterized for capacitance. Dielectric constants of the composites were determined by preparing four specimens in a slurry/paste form free from pores composed of different volume fractions of BT particles and polymer followed by filling the teflon cell with aluminum plate electrodes. The capacitance was measured at 1 MHz using HP 4284A Precision LCR Meter. The dielectric constant values (Ks) were calculated from the measured capacitance data using the equation 5.

$$C = \varepsilon_0 KA/t \quad (5)$$

Where ε_0 = dielectric permittivity of the free space, 8.854×10^{-12} F/m

A = area of the electrode and ceramic contact area, 1 cm^2

t = thickness of the ceramic specimen, 0.4 cm

The dielectric constant of all the samples was determined using the capacitance values. The values thus obtained were plotted and compared with the known theoretical models to make sure that this method is consistent and reliable.

Results & Discussion

Dielectric constant values of the different composite samples were calculated from the measured capacitance data using the equation 5. The dielectric constant values obtained by using castor oil as the second phase are plotted in Fig. 5.

The values using the polymer as the second phase are also obtained. These values are plotted against the theoretical models shown in Fig. 6. The values indicate that at 50 volume% of the ceramic the dielectric constant of the composite is 89 which is considerably higher than the values predicted by the theoretical models.

A composite with a higher volume% of the ceramic could not be fabricated as higher content of the filler leads to a non-uniform functional layer. Extrapolating the dielectric constant results that are plotted against the ceramic volume fractions in Fig. 5 gives the dielectric constant of ceramic particle as 178.

The experimental results of the dielectric constant values of the composite are plotted against the ceramic volume fractions in Fig. 7 and extrapolating this plot gives the dielectric constant of ceramic particle as 171. Both the composites with castor oil and the polymer show the dielectric constant values in the same range.

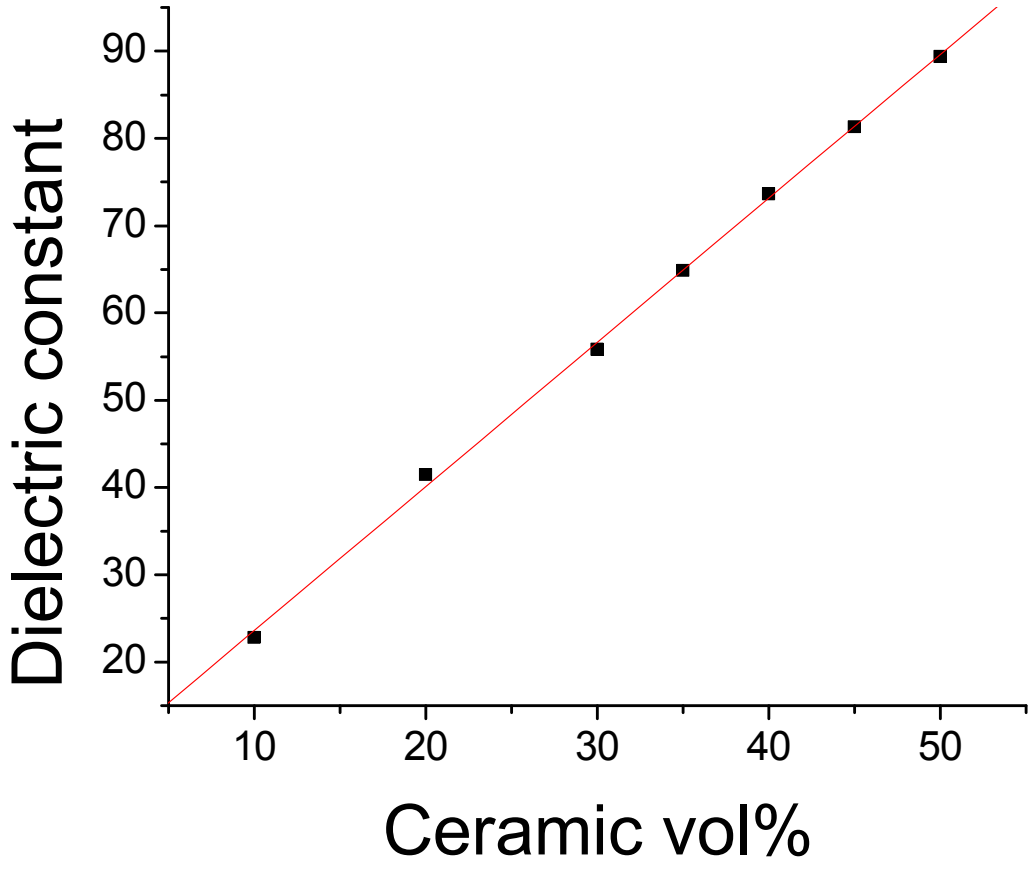

Fig. 5. Dielectric constant values vs. ceramic volume % (BT 8 & Castor oil)

The true value of permittivity of a statistic composite should lie between the values determined by Lichtenecker equation. The dielectric behavior of statistic systems has been analyzed by many scientists and many equations have been derived based on experimental results and theoretical derivation. The most commonly used equation is the Lichtenecker logarithmic law of mixing and is written for a two-component system as shown in equation 6 & equation 7 is a modified form of Lichtenecker equation, where k is a fitting constant subject to composite material. It is reported that k has a value around 0.3 for most well-dispersed polymer/ceramic composites [12].

$$\log \varepsilon = v_p \log \varepsilon_p + v_c \log \varepsilon_c \quad (6)$$

$$\log \varepsilon = \log \varepsilon_p + v_c(1-k) \log (\varepsilon_c/\varepsilon_p) \quad (7)$$

where v_p = volume fraction of polymer

v_c = volume fraction of the ceramic

ε_p = dielectric constant of the polymer

ε_c = dielectric constant of the ceramic

The logarithm of dielectric constant results are plotted against the ceramic volume fractions in Fig. 8.

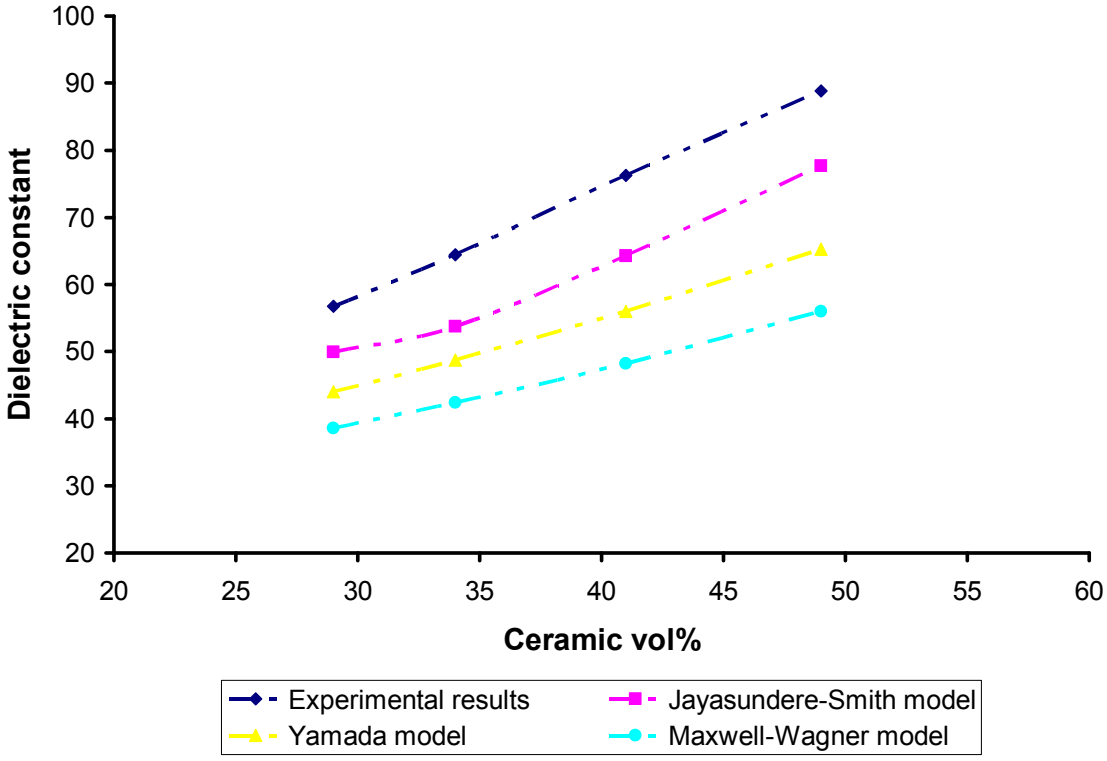

Fig. 6. Dielectric constant values vs. ceramic volume % (BT 8 & CEPVA with other theoretical models)

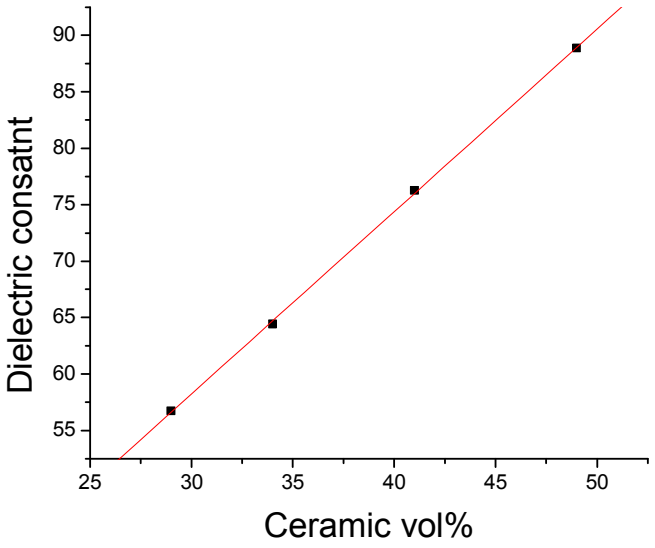

Fig. 7. Dielectric constant values of the composite vs. BT volume % (BT 8 & CEPVA)

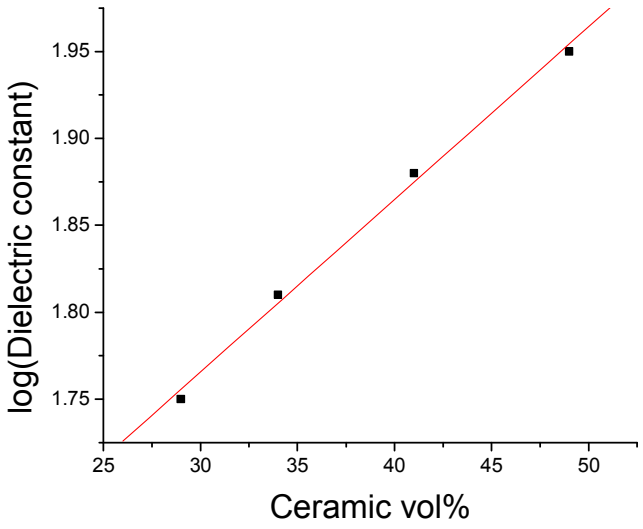

Fig. 8. log ε values of the composite vs. BT volume % (BT 8 & CEPVA – Lichtenecker model)

Based on this result, after linear fitting or extrapolating the curve the dielectric constants of the ceramic and the polymer were estimated and the results obtained were as follows.

ε_c = dielectric constant of ceramic, 170

ε_p= dielectric constant of the polymer, 21.7 ~ 22, which corresponds to the value provided by Plastpolymer J.S.Company in Russia. Using these dielectric constant values some predictions of the theoretical models have been considered for comparison.

Jayasundere and Smith [11] have worked together in deriving an equation which was modified from the well-known Kerner equation by including interactions between neighboring spheres for the measurement of dielectric constant of binary composites and the equation is shown in equation 8

$$\varepsilon_{eff} = \frac{v_p \varepsilon_p + v_c \varepsilon_c \left[\frac{3\varepsilon_p}{\varepsilon_c+2\varepsilon_p}\right]\left[1+\frac{3v_c(\varepsilon_c-\varepsilon_p)}{\varepsilon_c+2\varepsilon_p}\right]}{v_p + v_c \left[\frac{3\varepsilon_p}{\varepsilon_c+2\varepsilon_p}\right]\left[1+\frac{3v_c(\varepsilon_c-\varepsilon_p)}{\varepsilon_c+2\varepsilon_p}\right]} \quad (8)$$

where v_p = volume fraction of polymer

v_c = volume fraction of the ceramic

ε_p = dielectric constant of the polymer

ε_c = dielectric constant of the ceramic

The dielectric constant results are plotted against the ceramic volume fractions in Fig. 9 and extrapolating this plot gives the dielectric constant of ceramic particle as 161.

The Maxwell-Garnett mixing rule was initially used in a system where metal particles are encapsulated in an insulating matrix [13]. But in recent times the same mixing rule is applied for ceramic particle inclusions.

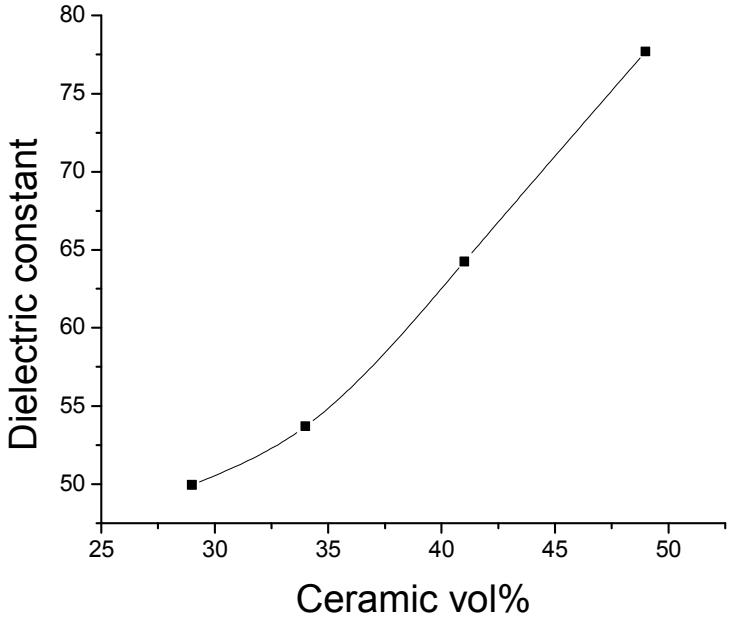

Fig. 9. Dielectric constant values vs. BT volume % (BT 8 & CEPVA – Smith model)

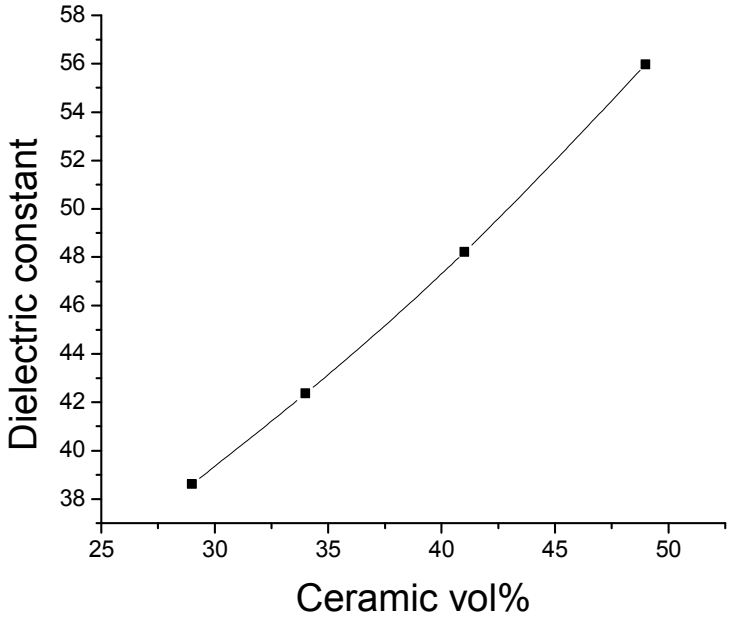

Fig. 10. Dielectric constant values vs. BT volume % (BT 8 & CEPVA – Maxwell model)

This mixing rule is then modified and the effective dielectric constant for a polymer/ceramic composite incorporating homogeneous distribution of spherical ceramic material can be determined by this equation developed by Maxwell and Wagner [12] which is known as Maxwell-Wagner mixing rule and is shown in equation 9.

$$\varepsilon_{\text{eff}} = \varepsilon_{\text{p}} \frac{2\varepsilon_{\text{p}} + \varepsilon_{\text{c}} + 2v_{\text{c}}(\varepsilon_{\text{c}} - \varepsilon_{\text{p}})}{2\varepsilon_{\text{p}} + \varepsilon_{\text{c}} - v_{\text{c}}(\varepsilon_{\text{c}} - \varepsilon_{\text{p}})} \tag{9}$$

where v_c = volume fraction of the ceramic

ε_p = dielectric constant of the polymer

ε_c = dielectric constant of the ceramic

The dielectric constant results are plotted against the ceramic volume fractions in Fig. 10 and extrapolating this plot gives the dielectric constant of ceramic particle as 110.

Yamada have studied the polymer/ceramic binary system and proposed a model using the properties of its constituent materials [10]. Considering the system to comprise ellipsoidal particles dispersed continuously, the dielectric constant is given by the equation 10.

$$\begin{aligned} \varepsilon_{\text{eff}} &= \varepsilon_{\text{p}} \left[1 + \frac{\eta v_{\text{c}}(\varepsilon_{\text{c}} - \varepsilon_{\text{p}})}{\eta\varepsilon_{\text{p}} + (\varepsilon_{\text{c}} - \varepsilon_{\text{p}})(1 - v_{\text{c}})} \right] \\ &= \varepsilon_{\text{p}} \left[1 + \frac{v_{\text{c}}(\varepsilon_{\text{c}} - \varepsilon_{\text{p}})}{\varepsilon_{\text{p}} + n(\varepsilon_{\text{c}} - \varepsilon_{\text{p}})(1 - v_{\text{c}})} \right] \end{aligned} \tag{10}$$

where n = 0.2, morphology factor depending on the shape of ellipsoidal particles on the surface of the film in his model.

v_c = volume fraction of the ceramic

ε_p = dielectric constant of the polymer

ε_c = dielectric constant of the ceramic

The dielectric constant results are plotted against the ceramic volume fractions in Fig. 11 and extrapolating this plot gives the dielectric constant of ceramic particle as 135.

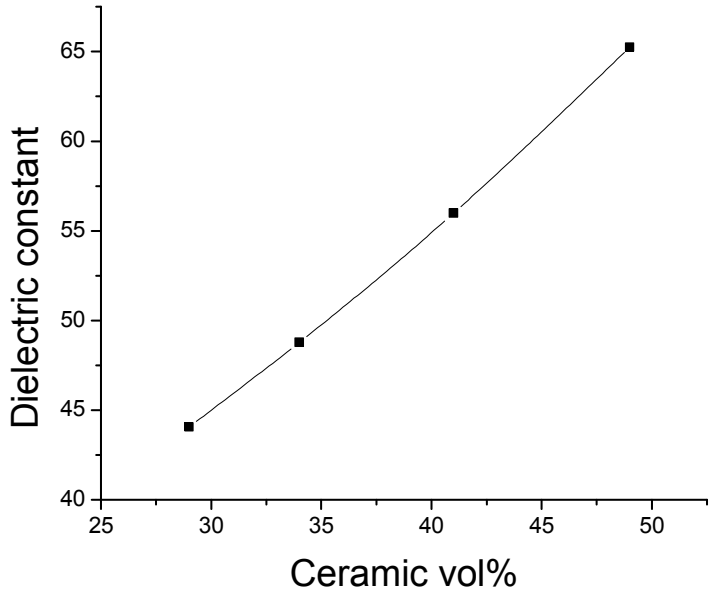

Fig. 11. Dielectric constant values of the composite vs. BT volume % (BT 8 & CEPVA – Yamada model)

Conclusions

After a thorough analysis of the results obtained, the dielectric constant values of these slurry composites calculated from the capacitance values are 0-35% higher than the values predicted by the most relied theoretical models. Hence the unique method that is developed and adapted in determining the dielectric constants of two phase polymer/ceramic composite is definitely useful in the prediction of electrical properties of such composites. Extrapolating these results, the dielectric constant of ceramic particles is observed to be 171 as calculated from this method while dielectric constant predicted by Lichtenecker, Smith, Maxwell-Wagner and Yamada are 170, 161, 110 and 135 respectively considering the values obtained are relative.

It is well-known that polymer/ceramic composites were synthesized, characterized and are widely used in various applications [27-29]. But majority of researchers considered epoxy as the second phase. The dielectric constant value was reported as 35 at 0.5 volume fraction of ceramic with modified high dielectric, low viscosity resin [27], 48 at 0.5 volume fraction of ceramic with photo-definable epoxies [28], 45 at 0.4 volume fraction of self-synthesized BT ceramic with epoxy [24], 65 at 0.6 volume fraction of BT with epoxy and the dielectric constant value falls down abruptly [8], and 45 at 0.6 volume fraction of BT which increased to 65 at 0.7 volume fraction of BT with epoxy [29]. Hence, by considering CEPVA as the second phase in this study, there was an increase in the dielectric constant value of the composite at the same volume fractions when compared to the values of the composites already known.

This method can also be used for a three phase composite considering the ratio of two phases to be constant. The precision and simplicity of this method can be exploited

for predictions of the properties of nanostructure ferroelectric polymer/ceramic composites.

Chapter 3

Dielectric Properties of Three-Phase Barium Titanate/Cyanoethyl Ester of Polyvinyl Alcohol/Silver Composites

Abstract

Three phase ceramic/metal/plastic (Cermetplas) percolative nanocomposites were prepared. A cyanoethyl ester of polyvinyl alcohol (CEPVA) was used as the base polymer to prepare the composites. Silver nanoparticles were prepared and used as the conducting phase. Nanocomposites of barium titanate particles embedded in CEPVA matrix, with silver as metallic inclusion, were characterized using the unique technique that was developed. The dielectric constant/permittivity, and loss tangent factor measurements were reported and discussed for Cermetplas composites below the percolation threshold. Experimental results show that a dielectric constant of above 320 could be achieved and the loss factor to be 0.05 below the percolation limit.

Introduction

Polymer/ceramic composites have drawn great interest recently as dielectric composite materials because of their ease of processability. There has been extensive research on these ceramic filled dielectric composites by many groups [30-35]. Need for high dielectric constant materials, makes it obvious to increase the ceramic loading in the polymer. But addition of ceramic itself will not help in achieving the requirements. Thus, metallic particles are introduced into the polymer/ceramic composite. On the other hand,

there have been reports of a high dielectric constant, but the metal/ceramic composites still need to be sintered at high temperatures [36-38].

In this study we report high dielectric constant values of three-phase composites. Silver has been introduced into the optimized polymer/ceramic matrix. The formulation for these composites was based on the effective dielectric constant prediction equations and the percolation theory [39-42]. Several researchers have found experimental evidence of an increase in the dielectric constant of the composite in the neighborhood of the percolation threshold [38,39,43-46]. A very high dielectric constant value can be obtained at conductive filler loading close to the percolation threshold taking care that the filler content does not exceed the threshold value. The percolation theory can be applied to analyze such composites when the metallic filler composition is close to the percolation threshold [29,30].

Metal particles can be polarized in the same way as dielectric ceramics, if insulated from the electrodes. In this case the polarization is caused by the electrons rather than ions. The only difference is that the polarization is caused by the displacement of free electrons rather than ions. Although the dielectricity of metal particles can not be characterized by the dielectric constant, it is this "dielectricity" (polarization) causes the enhancement of dielectric constant of the metal/polymer composites. This is the reason for metal/polymer composites showing increased dielectric constants [47-49]. Nevertheless, the accumulated polarization will disappear when the insulation between filler particles is broken by direct contact of particles or electron tunneling. The charge will be transported through the formed filler network to the electrodes. The probability of forming a giant particle network between the two electrodes is proportional to the particle

concentration, which is known as percolation [50]. As soon as such a conducting channel is formed, the free charges in fillers will merge with the outside current, and dielectricity is lost. For composites with conducting fillers, the occurrence probability of percolation will become nearly unity at certain filler concentration, which is known as the percolation threshold. The dielectric constants of conductor-insulator composites near the threshold were usually modeled by the scaling theory [50].

When a giant percolative particle cluster forms, a conducting network is formed between electrodes. The dielectric constant of the material will sharply decrease to almost zero and dielectric loss will be extremely high. Therefore, although high dielectric constants near the percolation threshold are attractive to researchers, the risk of percolation should also be considered for practical applications. Therefore, to utilize the divergent behavior of the dielectric constant of a metal/polymer composite for the dielectric applications, measures have to be taken to prevent the occurrence of percolation. For practical applications, it will be worthy to eliminate the risk of percolation.

In our study, nanoparticles of silver have been used, with an aim of forming a large number of microcapacitors to achieve higher dielectric constants. Silver was selected as the metal filler material because of several reasons. First, silver is an excellent conductor. Secondly, silver is a noble metal which can be easily reduced to form metal particles. Third, the chemical methods for preparing silver nanoparticles are well developed. Finally, the cost of silver is relatively lower than those for gold or platinum. These nanoparticles were synthesized with a surfactant layer on it which eliminates the difficulty in dispersion. CEPVA has been used as the matrix because of its better

toughness, chemical and thermal stability, and low coefficient of thermal expansion. Silver nanoparticles were synthesized for the preparation of ceramic/metal/polymer composites. The produced silver nanoparticles were coated with organic surfactant during the synthesis, which functions as a final barrier to prevent the particles from contacting each other. The surfactants also performed as both a size-controlling agent and a dispersing agent.

Materials & Procedures

The polymer/ceramic composites are prepared using the commercial ceramic powder, Cabot BT-8 (BT), (hydrothermal powder with a mean particle size of 0.2μm obtained from Cabot Performance Materials, Boyertown, PA), a cyanoethyl ester of polyvinyl alcohol (CEPVA) kindly provided by Plastpolymer J.S.Company via St. Petersburg State Institute of Technology, Russia, Castor oil, Eur. Pharm. grade, having a density of 0.957 g/cc obtained from Acros Organics and BYK-W 9010 from BYK-Chemie which is a dispersant used for a better dissolution of the ceramic powder. The silver nanoparticles were prepared by a method similar to those reported [51,52]. Silver nitrate was used as the silver precursor. Sodium borohydride (SBH) was used as the reducing agent. A mixture of mercaptosuccinic acid (thiol ligand) and dodecanoic acid (acid ligand) was used as the surfactant. All the chemicals were purchased from Aldrich. A pre-determined amount of silver nitrate, 2 g, was dissolved in 10 ml of distilled water. The thiol and acid ligands were dissolved in anhydrous methanol that was about 10 times in volume of the water used above. The molar ratio of thiol ligand to acid ligand was set to 1:4.5. The molar ratio of thiol ligand to silver varied from 2:1 to 1:100. The silver

solution was then mixed with ligand solution under stirring. Freshly prepared SBH methanol solution was added into the silver solution dropwise. Dark brown color appeared instantly upon the adding of SBH and the whole solution became dark red or black after the addition. The molar ratio of SBH to silver was set to 1:2.

The reacting solution was kept under stirring for 10 more minutes after the addition to fully reduce silver. The dark precipitate was separated by centrifugation and the supernatant liquid was decanted. The precipitated silver nanoparticles were then refluxed in methanol for 15 minutes. After refluxing, silver particles were precipitated by centrifugation. The refluxing-centrifugation cycle was repeated in methanol for three times to remove the extra organic and inorganic ions and the silver particle size was estimated to be around 50 nm.

The same polymer/ceramic composite that was discussed about in chapter 2 was considered with a 0.8 weight fraction of the ceramic. The reason for considering that particular composite was because it was observed to have the maximum dielectric constant value among all the samples prepared. The procedure for preparing the polymer and ceramic suspensions was the same as followed in our earlier work [54]. Synthesized silver particles were introduced into the polymer/ceramic suspensions. Then the suspension is ball-milled for 12 hr. The prepared mixtures were then gently dried at 80°-90° C under both continuous magnetic stirring and mildly reduced pressure to get rid of the solvents where viscous slurries/pastes were obtained. The dried composites were then kept under reduced pressure and used for further characterization.

The capacitor is fabricated using the same procedure that was followed in our earlier work [53,54] and is characterized for capacitance. Dielectric constants of the

composites were determined by preparing four specimens in a slurry/paste form free from pores composed of different volume fractions of BT particles and polymer followed by filling the teflon cell with aluminum plate electrodes. The capacitance was measured at 1 MHz using HP 4284A Precision LCR Meter. The dielectric constant values (Ks) were calculated from the measured capacitance data using the equation 11

$$C = \varepsilon_0 KA/t \quad (11)$$

where ε_0 = dielectric permittivity of the free space, 8.854 X 10^{-12} F/m

A = area of the electrode and ceramic contact area, 1 cm^2

t = thickness of the ceramic specimen, 0.4 cm

The dielectric constant of all the samples was determined using the capacitance values. The values thus obtained were plotted and compared with the known theoretical models to make sure that this method is consistent and reliable.

Results & Discussion

Dielectric constant values of different composite samples were calculated from the measured capacitance data using the equation 11. Fig. 12 is the plot of dielectric constant of the Cermetplas composites as a function of the silver volume fraction. The dielectric constant of Cermetplas composites increased gradually from 89 (the dielectric constant of BT/CEPVA composite with 0.8 wt. fraction of ceramic) to above 320 at 1 MHz and room temperature with a silver volume fraction up to 30 vol%. The dielectric constant then started decreasing with further addition of silver. The origin of the increase of effective dielectric constant can be intuitively explained by the polarization of silver

particles within the CEPVA matrix under the electric field. The dielectric constant of the composite shows a curve similar to that follows the general material-mixing rule.

When the filler concentration is low, the average distance between silver particles is relatively large. When the filler concentration increases, the distance between particles decreased and the coupling of the induced polarization between silver particles become stronger. Thus the dielectric constant of composites goes up. In a classic model, when the filler concentration increases to a certain critical value, a giant cluster forms between electrodes and the coupling of the polarization in fillers reach the maximum. Thus, an almost infinitely high dielectric constant will result. When the filler concentration increases beyond the critical value, the coupling is so strong that the insulation between particles is broken and a conducting channel is formed. So, the dielectric constant decreases to nearly zero.

However, in this work, silver nanoparticles were enveloped in a thin layer of organic surfactants, which set the minimum distance between the particles. Thus, the particles can not directly touch each other even without the matrix. As a consequence, the synthesized Cermetplas composites did not show very sharp increase of the dielectric constant at a certain concentration.

The dielectric constant of Cermetplas composites increased more smoothly and formed a broad peak between 15 vol% and 35 vol%. This slow but broad increase of dielectric constant demonstrates a high concentration tolerance, which reduces the risk of conductive percolation. The dielectric loss factor values are plotted in Fig. 13 which indicates a sudden increase in the loss factor with increase in silver volume% above the percolation threshold. According to Lai Qi [55], Cermetplas with epoxy matrix showed a

similar broad peak and the percolation limit was observed at 22.5 vol% of the silver content. The effective dielectric constant value of the epoxy composite at 30 vol% silver was 316.7 whereas the dielectric constant value of our CEPVA composite at 30 vol% was 320. Though we have used a polymer, CEPVA with a relatively high dielectric constant than epoxy, the effective dielectric constant of the composite showed almost the same value. With this evidence we might predict or assume that the polymer matrix just acts as a binder phase in a 3-phase composite.

This characteristic makes the Cermetplas composites suitable for practical applications. The decrease of dielectric constant of the Cermetplas composites with increasing frequency was due to the slower dielectric relaxation of CEPVA at higher frequency.

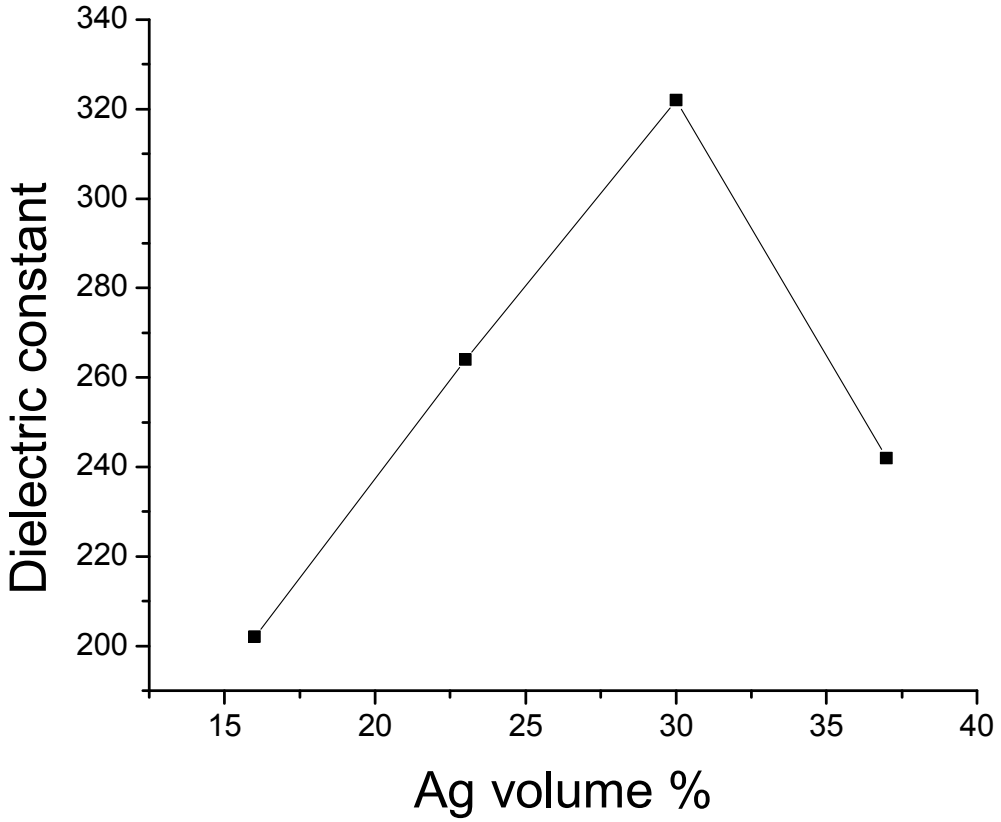

Fig. 12. Dielectric constant values of Cermetplas (0.8 wt. fraction BT) vs. silver volume%

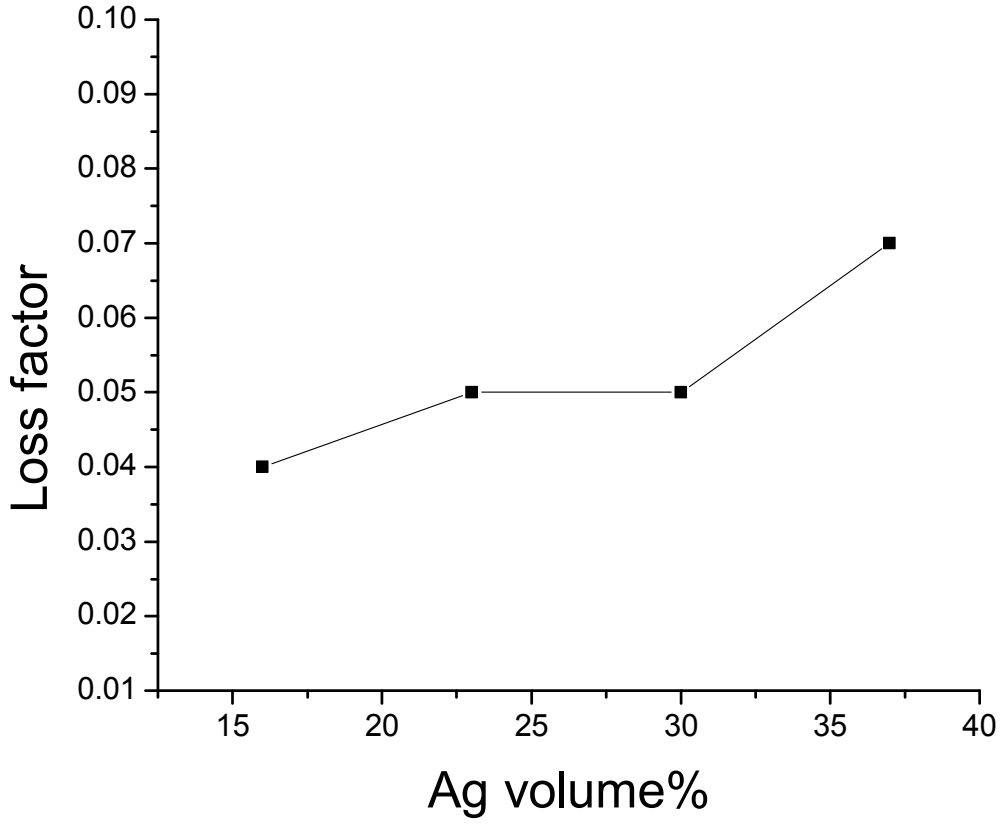

Fig. 13. Loss factor values of Cermetplas (0.8 wt. fraction BT) vs. silver volume %

When the silver volume fraction increased to about 30 vol%, the dielectric constants of Cermetplas composites started decreasing with further addition of silver. The reason was the introduction of porosity into the composites. Due to the absorbed surfactants, there is space between silver particles even in the powder state. When the amount of silver is small, CEPVA is enough to fill the space. When the amount of silver increases to certain value, CEPVA is not enough even to fully occupy the space between particles. Thus, the porosity of the composites increases.

After the refluxing treatments, the dried silver nanoparticle lump has a volume about 6-7 times larger than the theoretical value. This renders a density only 20-25% of the density of the pure silver (10.5 g/cm^3). Therefore, the maximum loading of silver is approximately 35 vol%. A volume fraction above this value is not practically achievable, even with a higher Cermetplas weight ratio. In other words, when the CEPVA amount was right enough to just occupy the space between particles, the composite reached the maximum silver volume fraction. Further adding silver caused the introduction of air, which will decrease the relative density and dielectric constant of the composite.

Conclusions

The Barium titanate/silver/CEPVA Cermetplas composites were successfully prepared. Characterization of their dielectric properties was performed. The dependence of dielectric constant and loss on the conducting filler content was studied. The dielectric constant of the composites can be enhanced greatly by introducing metal particles in it. Processing ease and flexibility to make capacitors, and high dielectric constant, makes Cermetplas candidates for a wide variety of energy storage applications. Barium

titanate/silver/CEPVA Cermetplas showed a dielectric constant of more than 320 at room temperature. This value is among the highest dielectric constants reported. The dielectric loss of prepared Cermetplas is also relatively low. The technique followed in fabricating the capacitor for characterizing the dielectric properties definitely works for a three phase composite.

Chapter 4

Effect of Lattice Hydroxyl on the Phase Transition and Dielectric Properties of Barium Titanate Particles

Abstract

Presence of the hydroxyls in the lattice is believed to be the major cause of the reduced tetragonality in the barium titanate ceramic powder. Commercial barium titanate that is known to be cubic in nature has been used in this study. This sub-micron powder is treated with N-Methyl-2-Pyrrolidinon (NMP) to obtain a tetragonal powder as confirmed by x-ray diffraction analysis, differential scanning calorimetry and the c/a ratio. The dielectric constant of a single particle of this NMP treated cubic powder is reported to be around 64% higher than the as-received cubic powder. To add weight to the hypothesis mentioned hitherto, simulation experiments have been performed by preparing acidic water, with a pH~3-4 and in basic water, with a pH~12-13. The as-received cubic barium titanate powder, calcined at different temperatures, has been aged in different pH conditions, acid and basic waters. Then the powder is further used for the characterization of electrical properties. The dielectric properties of the barium titante ceramic powder that is determined does depend inversely on the lattice OH content as confirmed by FTIR spectroscopic analysis and TGA results.

Introduction

The miniaturization of the electronic devices and electronic components has received phenomenal interest in the prospects of future technology [56-60]. The perovskite type structured barium titanate which is a metal oxide exhibits outstanding chemical and physical properties, such as catalysis, oxygen-transport, ferroelectric, piezoelectric and dielectric behavior [61-63]. High values of the dielectric constant and low loss factor of barium titanate make it a particularly desired material from which capacitors, condensers, resistors, insulators and other electronic components can be fabricated [64-70].

The high value of dielectric constant of barium titanate particle arises due to the high polarizability of its relatively simple lattice structure in which small Ti^{+4} ions have relatively more space within the oxygen octahedra [71]. It was well known that the stability of the unit cell strongly depends on the size of the crystals and the Curie temperature, 130°C. Below the curie temperature, the Ti^{+4} ions occupy off-center positions, which results in the change of crystal structure from cubic to tetragonal [72-74]. This displacement is the origin of the room-temperature ferroelectricity and piezoelectricity of barium titanate and other perovskite oxides.

The values of the dielectric constant of the barium titanate also change accordingly depending on the size and the crystal phase. The dependence of dielectric constant on the particle size of barium titanate has been already reported [65,66,75]. The synthesis of barium titanate via hydrothermal process is carried out in excess water content at very high OH concentration [76,77]. Therefore, it is evident that some OH groups may be entrapped in the crystal lattice. The adverse effects of the entrapped OH

groups have been well documented [78-83]. No method other than heating has been reported so far, which can effectively extract the lattice hydroxyls. Also, experimental evidence of the lattice impurity effect on the cubic–tetragonal transition has been reported [84-86]. However, a clear understanding of the nature of the incorporation and mechanism of removal of these species is still lacking.

Lattice hydroxyl groups are the most well-known lattice impurity in barium titanate, which cause cationic vacancies, enlargement of unit cell and sintering difficulty. Our previous study showed that OH extraction could be achieved by treating the hydrothermal barium titanate powder in Dimethyl Formamide [87]. The dielectric properties were significantly improved. By changing the reaction media from a water-providing type to a water-extracting one, the water molecules can be extracted from the crystallites by diffusing and dissolving in a highly polar, high boiling point organic liquid.

It has been reported that OH groups adsorbed on the surface of the barium titanate powder exhibit an infrared absorption because of the availability of many different surface adsorption sites [88]. However, in the case of hydrothermal barium titanate powders, a relatively sharp peak occurring at a similar wave number 3496 cm^{-1} was observed by Noma et al. [89] and attributed to the absorbance of OH groups incorporated into the barium titanate ceramic lattice. The broad OH resonance was almost eliminated only after calcining the barium titanate powder for 1 h at 600–800 °C, as observed in previous studies. It is also observed that there will be a band height increase at 600ºC which is explained by the diffusion of the incorporated lattice hydroxyl ion to the surface of the barium titanate particles [67,89-91]. There is an appreciable amount of lattice

incorporated protons and hydroxyl ions present in hydrothermally synthesized barium titanate powder and it is found that this lattice OH diffuses to the surface by the process of annealing [80,87].

Some information on the presence and location of OH groups has been obtained using a variety of techniques, including infrared analysis, FTIR and TGA which have been used to further elucidate the nature of lattice hydroxyl groups in hydrothermal barium titanate powder ceramics. The formation mechanism and the effect of hydroxyl ion on the dielectric properties of the barium titanate nano-crystals were not explored till date. Therefore, our present investigation involves the reporting the chemical treatment of converting nanocrystalline cubic barium titanate to tetragonal phase without particle growth. The results are then related to dielectric properties.

Materials & Procedure

A commercial grade barium titanate, Cabot BT-8 , (hydrothermal powder with a mean particle size of 0.2μm obtained from Cabot Performance Materials, Boyertown, PA), was used in the present work. A highly polar solvent N-Methyl-2-pyrrolidinon (NMP), (bearing a density of 1.03 g/cc obtained from Acros Organics), was used to extract OH ions, Castor oil, (Eur. Pharm. grade, having a density of 0.957 g/cc obtained from Acros Organics), acetic acid, CH_3COOH (glacial with 99.7% purity obtained from Fisher products) and potassium hydroxide, KOH (flakes obtained from Aldrich). The solvent was used without any prior treatment and purification.

The commercial BT that retains a cubic phase was initially estimated for a definite amount of 5 g in a closed teflon jar. A pre-determined amount, 75 ml of NMP

was then added to the teflon jar. The mixture or the suspension was thoroughly agitated at a temperature of 200ºC for 24 hr on a magnetic stirring hot plate. Then the obtained sol was centrifuged to remove the solvent, washed with diluted CH_3COOH and then with water and ethyl alcohol alternately. The washing process was repeated for three times. The collected powder was then dried under vacuum at 90ºC only to remove the excess surface water and solvent present leaving a pure barium titanate powder behind. The crystallinity and the tetragonal phase transformation were confirmed by the x-ray diffractometry.

As discussed, the major constituent in this type of cubic-to-tetragonal phase transformation is due to the elimination of OH ions present in the lattice. Simulation experiments have been done to elaborate the concept. 200 ml of deionized water was taken in two different beakers each of 100 ml. We prepared the water in one beaker with CH_3COOH maintaining a pH around 3-4 and naming it as acidic water whereas the other beaker of water with KOH maintaining a pH around 12-13, naming it as basic water. The commercial cubic phase barium titanate was introduced as three different samples. The first sample – as-received and at room temperature, the second sample – as-received and calcined at 200ºC, and the third sample – as-received and calcined at 1100ºC. Each sample was exactly estimated to 10 g, 5 g for acidic water and 5 g for basic water respectively. Once the samples were ready, they were aged for 24 hr in the different pH waters at room temerature. Then the samples were dried under vacuum at 90ºC only to remove the excess surface water content.

After the x-ray diffraction analysis and other thermal analysis methods, the samples were used for the determination of the dielectric properties using the capacitor

technique. Initially, castor oil and the NMP treated barium titanate ceramic powder was mixed in different proportions. These mixtures had a variable ceramic content of 10-50% by volume on the dry basis. Then castor oil was mixed with the differently aged barium titanate ceramic powder samples one-by-one. These mixtures had a variable ceramic content by volume on the dry basis. All these samples were ready for the characterization. The capacitor was fabricated using the same procedure that was followed in our earlier work [53,54] and the samples were characterized for capacitance and loss factor. Dielectric constants of all the ceramic powders were determined by preparing a slurry/paste form free from pores composed of different volume fractions of barium titanate particles and castor oil followed by filling the teflon cell with aluminum plate electrodes. The capacitance was measured at 1 MHz using HP 4284A Precision LCR Meter. The dielectric constant values (Ks) were calculated from the measured capacitance data using the equation 12.

$$C = \varepsilon_0 KA/t \quad (12)$$

Where ε_0 = dielectric permittivity of the free space, 8.854×10^{-12} F/m

A = area of the electrode and ceramic contact area, 1 cm^2

t = thickness of the ceramic specimen, 0.4 cm

The dielectric constant of all the samples was determined using the capacitance values.

Results & Discussion

This method is a low-temperature solvothermal treatment of hydrothermal commercial barium titanate powders in a polar solvent, NMP in a sealed teflon jar. Fig. 14 shows the XRD pattern, in the 2θ range of 35-55 for the NMP treated barium titanate

particles at 200ºC for 24 hr along with the XRD of untreated barium titanate particles. The tetragonality of barium titanate crystal is characterized by measuring the broadening of the {200} peaks. Before the NMP treatment, there was no appreciable broadening of the {200} peaks. When the samples were treated for 24 hr, a noticeable peak splitting is clearly observed at $2\theta = 45º$.

The peak splitting value and the c/a ratio were determined using the {200} peaks through the single peak deconvolution approach. The c/a ratio changed from 1.001 (as-received) to about 1.0078 after samples were treated in NMP at 200ºC for 24 hr. Considering the theoretical tetragonal asymmetry (c/a =1.01) [92] and the fact that tetragonal and cubic phases always co-exist in barium titanate crystals, it is very much obvious to conclude that the NMP treated barium titanate particles were tetragonal. The enhanced tetragonality was also confirmed by the DSC results, a curie transition at 133ºC, as shown in Fig. 15. Before the NMP treatment, the barium titanate particles were cubic at room temperature and showed no phase transformation in DSC upon heating up to 200ºC.

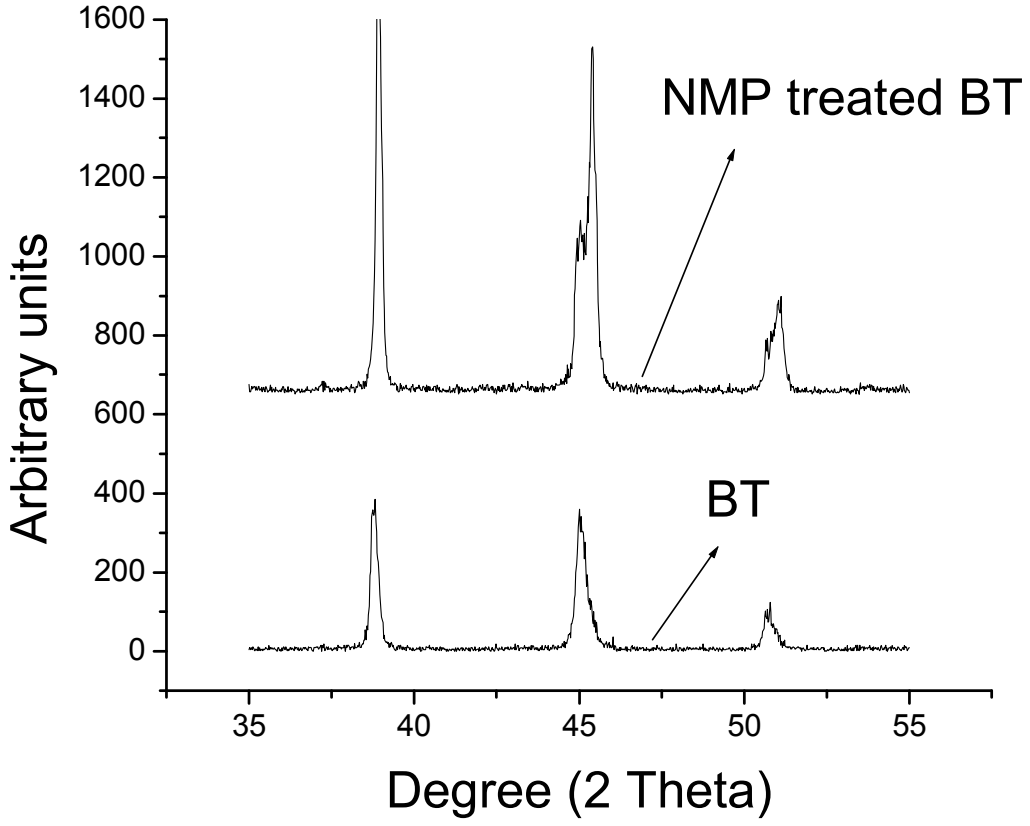

Fig. 14. Partial XRD pattern of BT – before and after NMP treatment (NMP treatment showing the peak split at 45º)

The hydroxyl content in the as-received, aged and NMP treated barium titanate particles was determined by FTIR analysis and TGA. Fig. 16 shows the FTIR spectrum of NMP treated barium titanate along with the untreated powder. The intensity of this broad peak in the range of 2600 - 3600 cm^{-1}, which is assigned to the OH stretching vibration, was significantly reduced after the NMP treatment. The presence of some barium carbonate was also detected in as-received powders, which was also removed by the treatment. It is necessary to distinguish lattice hydroxyls from the naturally absorbed surface water because surface water does not cause lattice strain. The semi quantitative comparison of the band intensities show that the lattice OH content in this NMP treated barium titanate powder to be 0.35%.

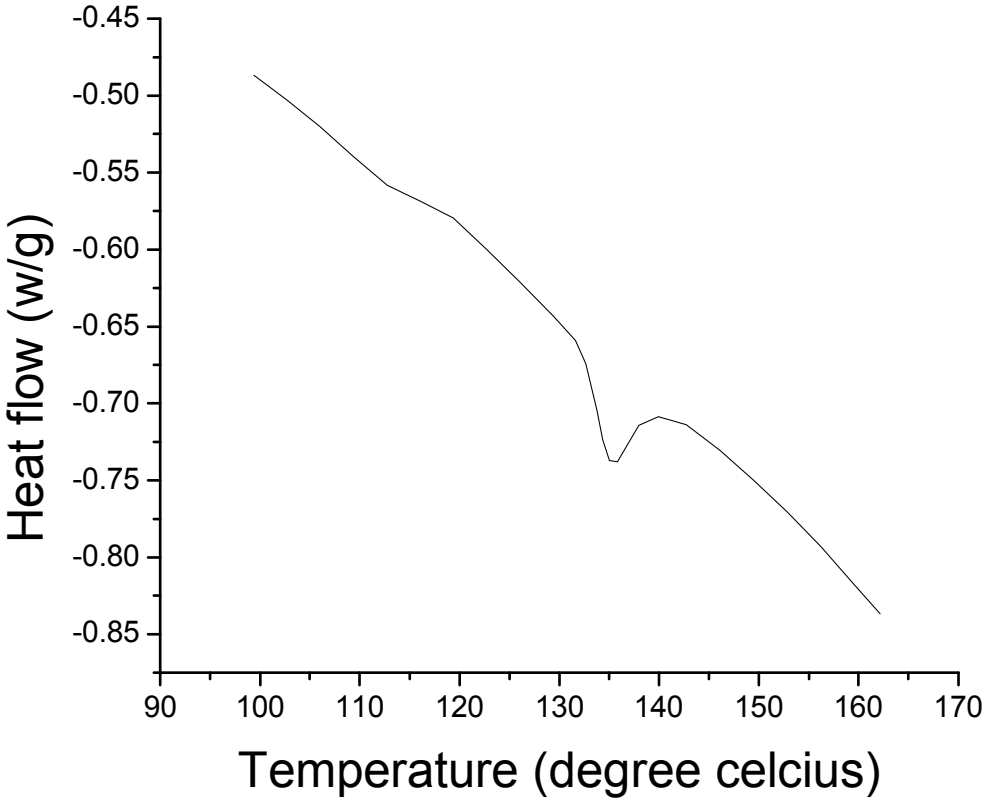

Fig. 15. DSC curve showing the tetragonal-to-cubic transition in the NMP treated barium titanate powder during the process of increasing the temperature

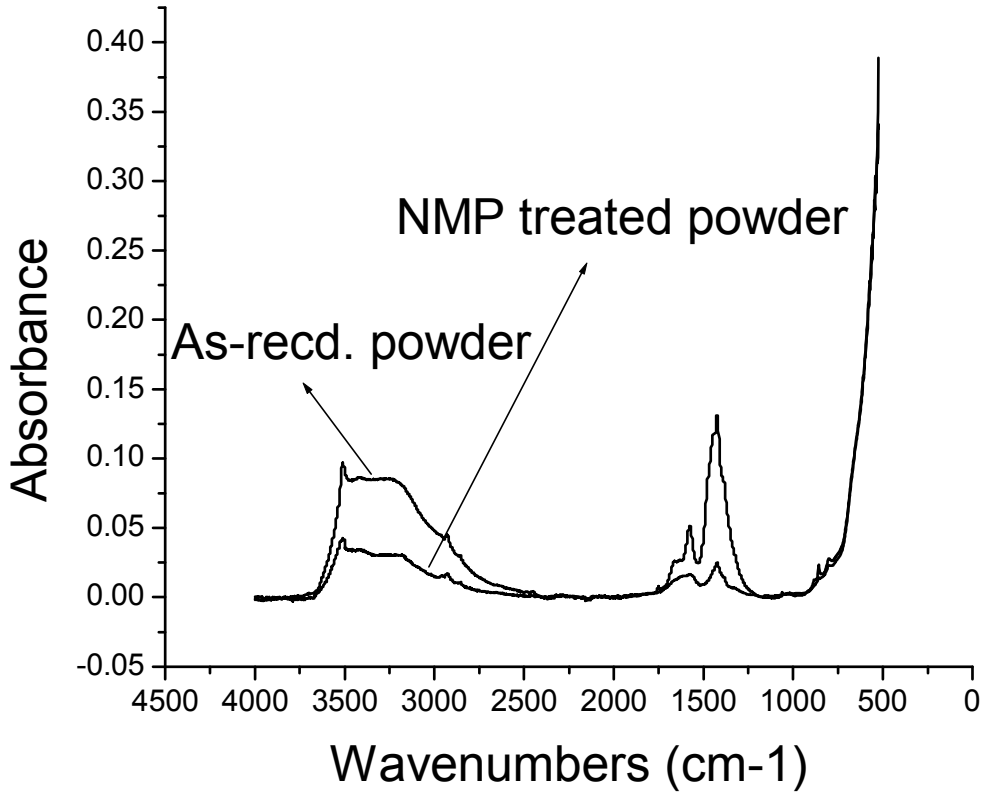

Fig. 16. FTIR spectra of barium titanate – before and after NMP treatment showing the OH vibration at 2600 – 3600 cm^{-1}

FTIR spectra, in the OH stretching region, of hydrothermal barium titanate powder calcined in air for 24 hr at room temperature, 200 and 1100 °C are shown in Fig. 17. The broad spectrum attributable to OH groups decreases with increasing the calcining temperature. The spectrum of the BT powder aged in different pH waters has two sharp peaks, a larger peak at 3496 cm^{-1} corresponding to the surface OH and a smaller peak at 2931 cm^{-1} that corresponds to the peak position observed for the lattice OH, of 1426 and 1469 cm^{-1} to lattice and surface carbonate respectively and of 785 and 545 cm^{-1} to barium titanate.

Semi quantitative comparison of the species by band intensity of OH at 2931 cm^{-1} was calculated to the ratio of the species by band intensity of barium titanate at 545 cm^{-1}. The observed lattice OH content in both the different pH waters is tabulated in Table 2.

The TGA results obtained were analyzed for the weight loss in each sample. It is generally considered that the total weight loss as a combination of weight loss of hydroxyl ions, both surface and lattice, and carbonate ions. Based on these results, a study is being done on the TGA curves, shown in Fig. 18, for the exact temperature range and the amount of weight loss of the lattice OH content.

It was already mentioned that between the temperature 250 – 450ºC, the incorporated lattice hydroxyl ion diffuses to the surface [80]. Hence, at that particular temperature range the slope and the weight loss are being calculated and the results are tabulated in Table 3.

It is clearly evident that as the temperature increases the amount of water and hydroxyl groups deplete. Both the results from FTIR and TGA support the earlier statement.

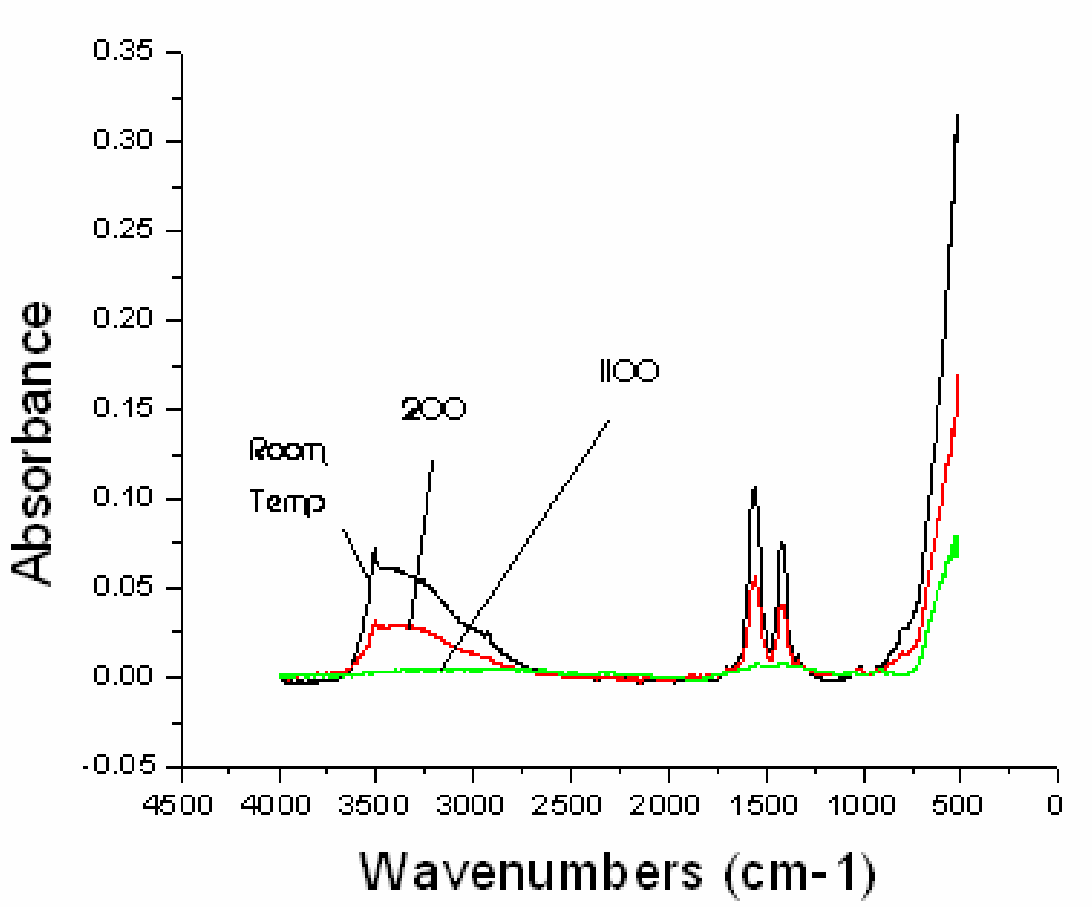

Fig. 17a. FTIR spectra of calcined barium titanate aged in acidic water

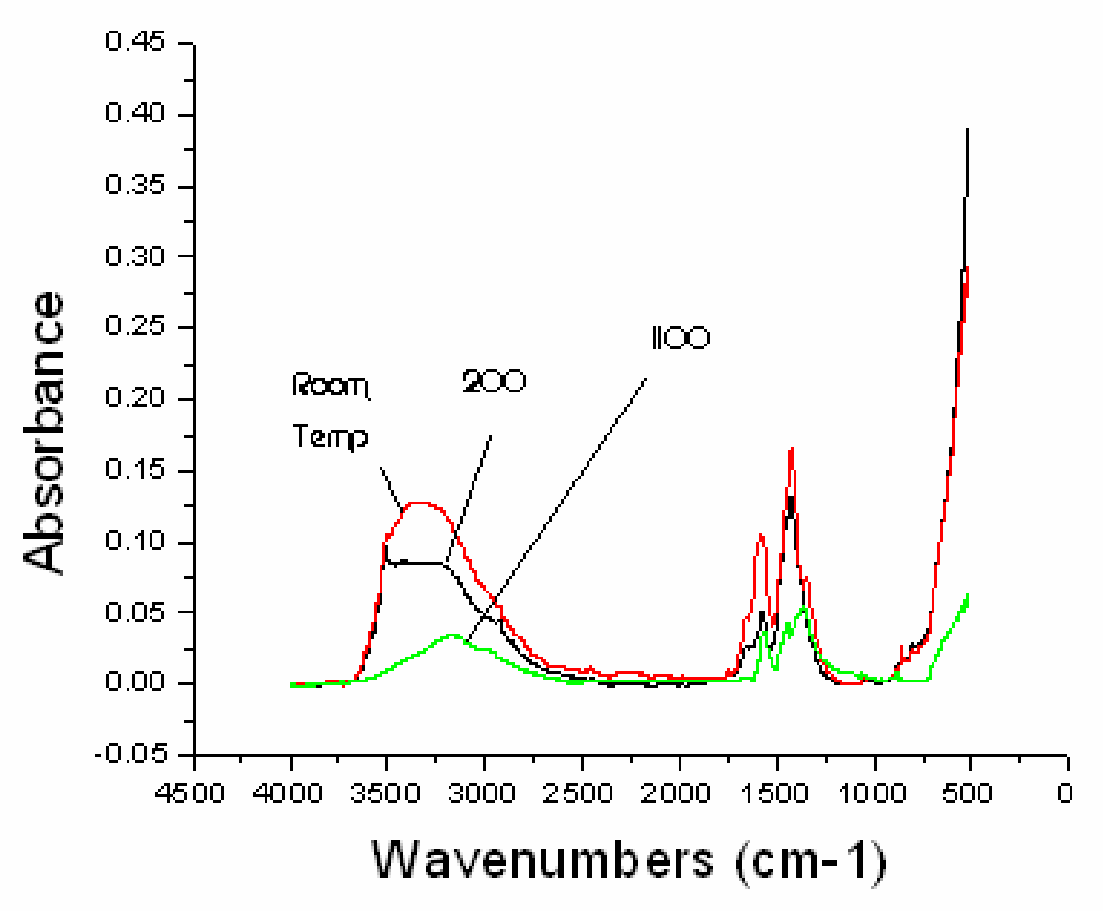

Fig. 17b. FTIR spectra of calcined barium titanate aged in basic water

Table 2. Amount of lattice OH content with respect to temperature aged in acidic and basic waters based on FTIR analysis.

Acidic water		Basic water	
RT	0.733 %	RT	2.213 %
200 ºC	0.599 %	200 ºC	2.022 %
1100 ºC	0.125 %	1100 ºC	0.385 %

Now it is very much understood that lattice OH plays an important role in phase transformation of barium titanate. The effect of the lattice OH content can be more clearly estimated by performing a dielectric study on the NMP treated barium titanate as well as the samples aged in different pH waters.

Dielectric constant values of the different samples were calculated from the measured capacitance data using the equation 12. The dielectric constant and loss values of the NMP treated barium titanate powder particles obtained by using castor oil as the binder phase is plotted in Fig. 19 and extrapolating this plot gives the dielectric constant of the NMP treated ceramic particles as 291 and the dielectric loss factor to be 0.03. Using the same technique, the dielectric constant value of the as-received powder particles is found to be 177 that were reported by our earlier work [53]. The dielectric constant of the commercial tetragonal powder particles, BT 219-6, in as-received condition is determined as 306 using the same procedure that was followed in our previous work [53,54].

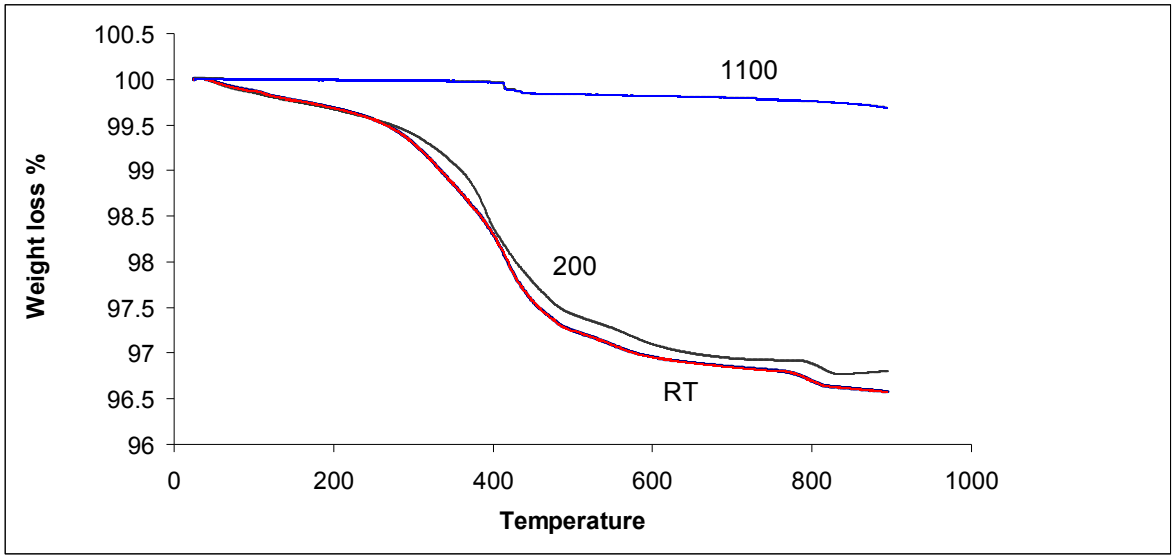

Fig. 18a. TGA curves for barium titanate aged in acidic water

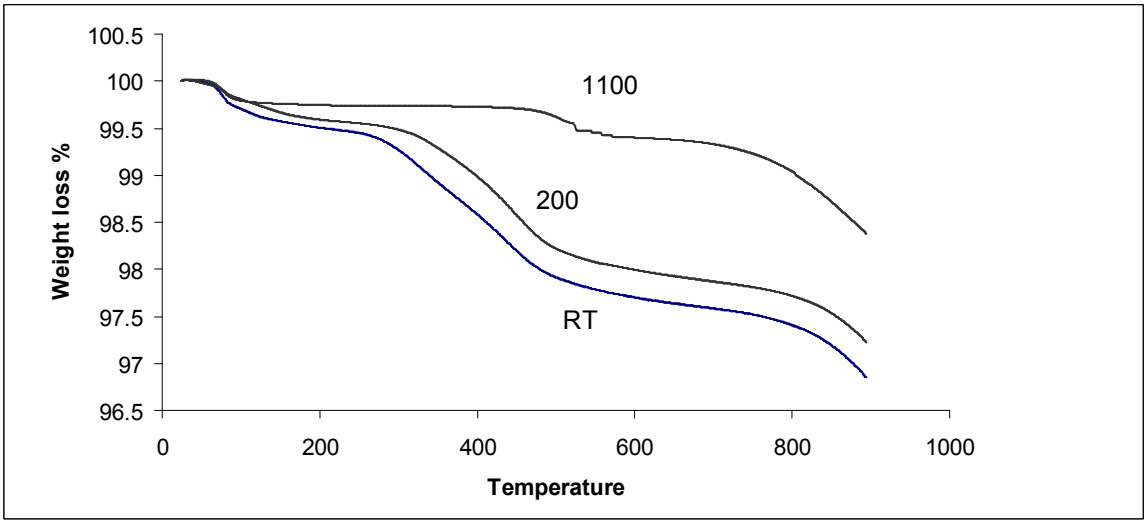

Fig. 18b. TGA curves of barium titanate aged in basic water

Table 3. Amount of lattice OH content with respect to temperature aged in acidic and basic waters based on TGA results.

Acidic water		Basic water	
RT	0.602 %	RT	1.989 %
200 ºC	0.577 %	200 ºC	1.887 %
1100 ºC	0.183 %	1100 ºC	0.312 %

Similarly the dielectric constants of all the six samples that were aged in different pH waters were being determined using castor oil as the binder phase. Then the dielectric constant results were plotted against temperature and lattice OH content that are shown in Fig. 20 and Fig. 21 respectively. The dielectric constant values of samples aged in acidic water give higher values due to smaller amount of OH content present in them when compared to the samples aged in basic water. The loss factor for both acidic and basic waters was increased by a very small amount. It was observed that there was an excess weight loss in the powder aged in basic water. The reason for this behavior was the instability on the surface of the particle. There was a definite amount of carbonate as well as OH present on the surface when compared to the powder aged in acidic water.

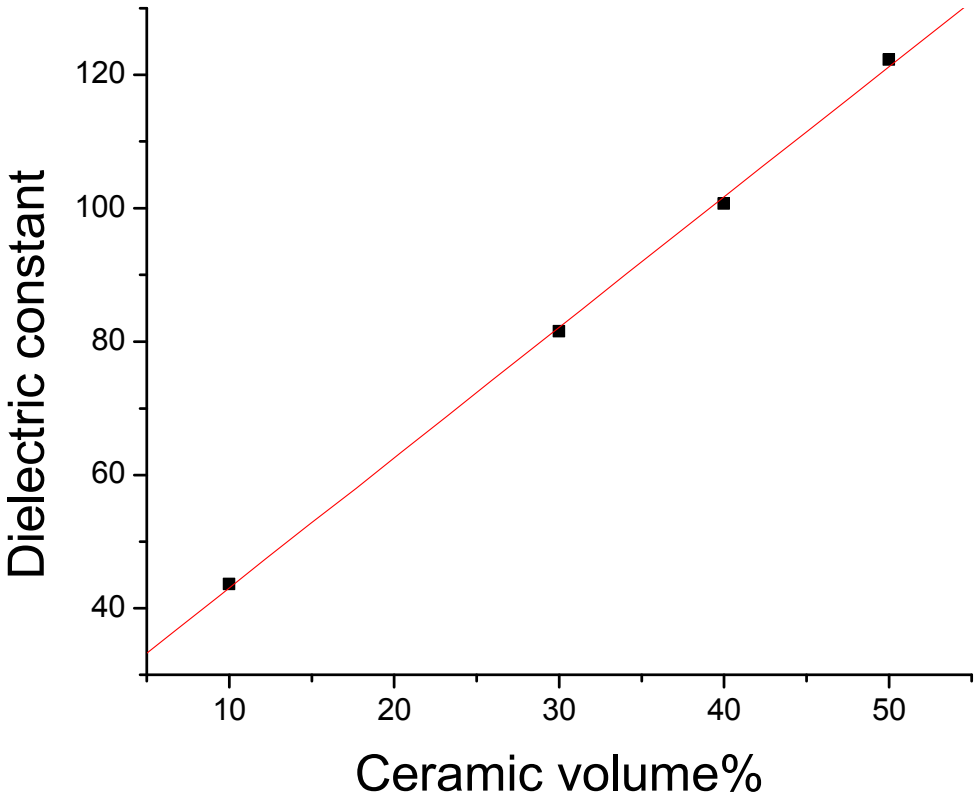

Fig. 19. Dielectric constant values of NMP treated barium titanate vs. ceramic volume %

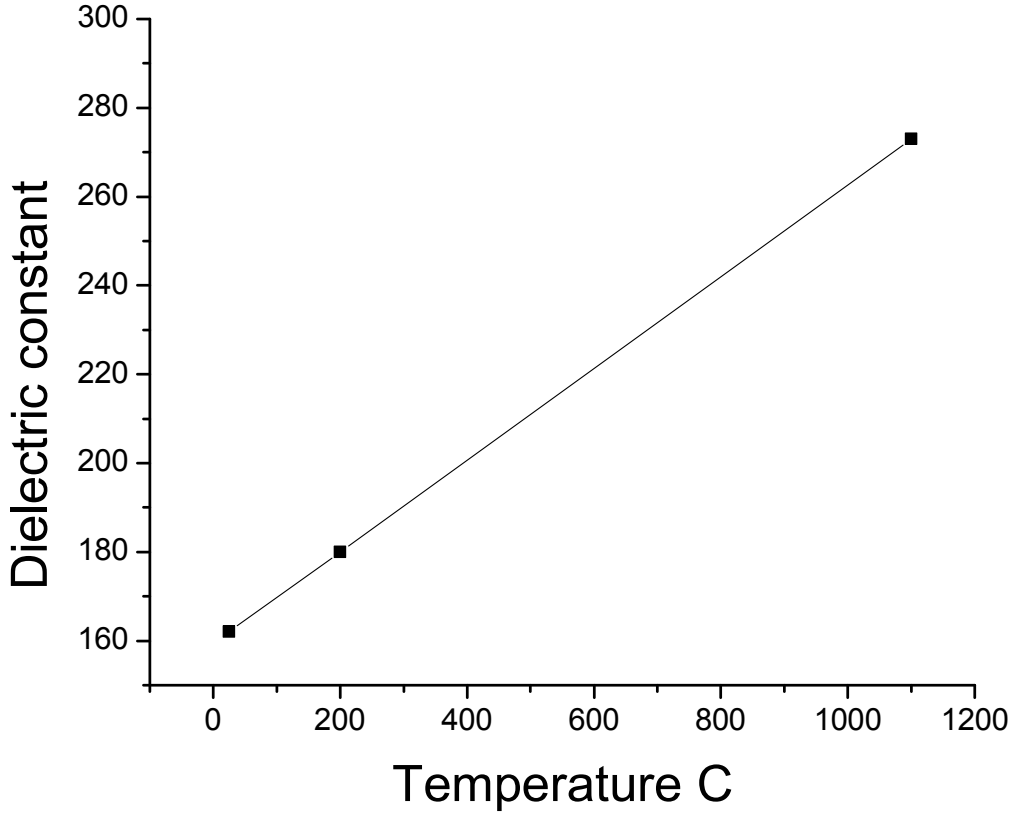

Fig. 20a. Dielectric constant values of barium titanate aged in acidic water as a function of calcining temperature

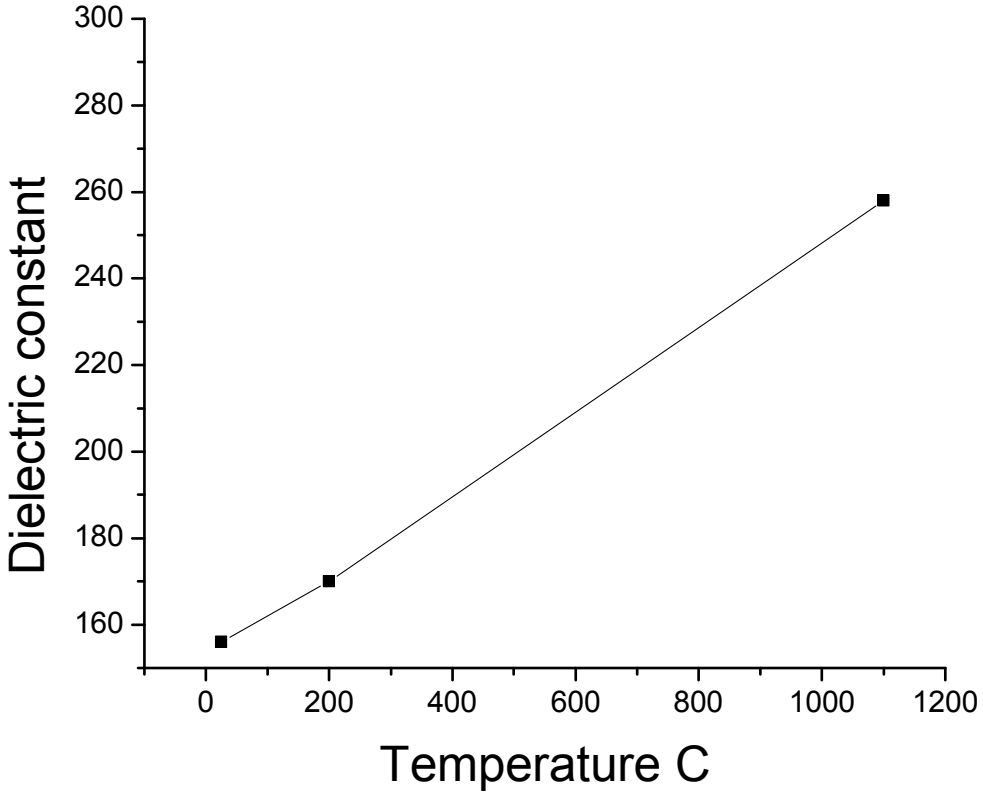

Fig. 20b. Dielectric constant values of barium titanate aged in basic water as a function of calcining temperature

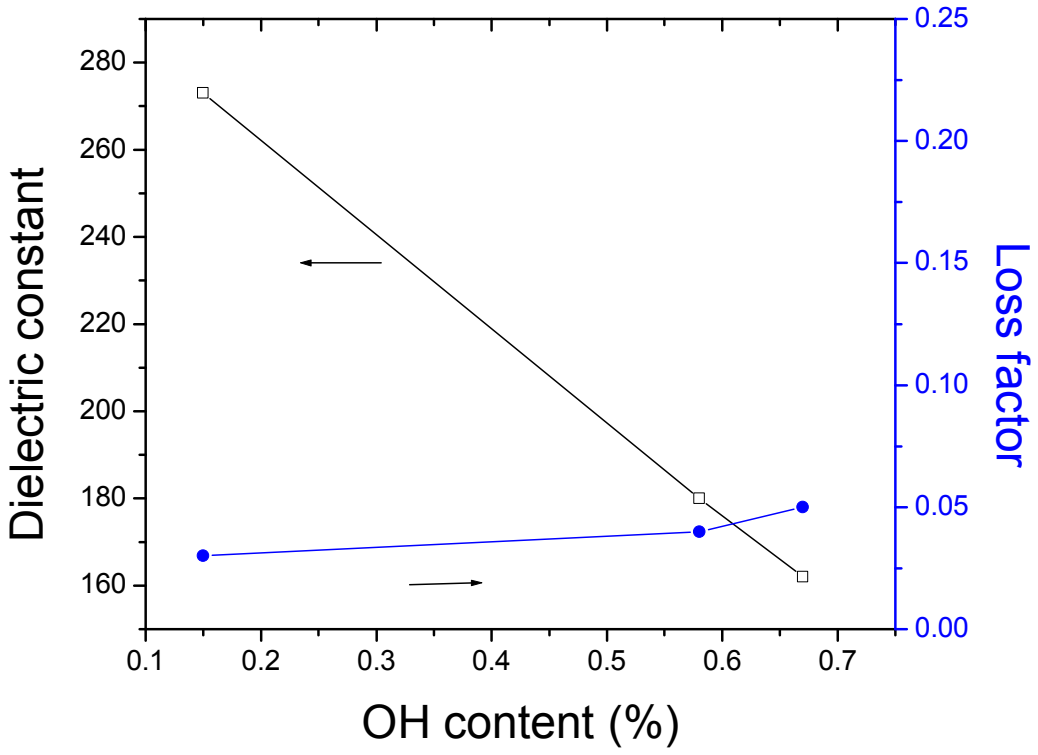

Fig. 21a. Dielectric properties of barium titanate aged in acidic water with increasing OH content

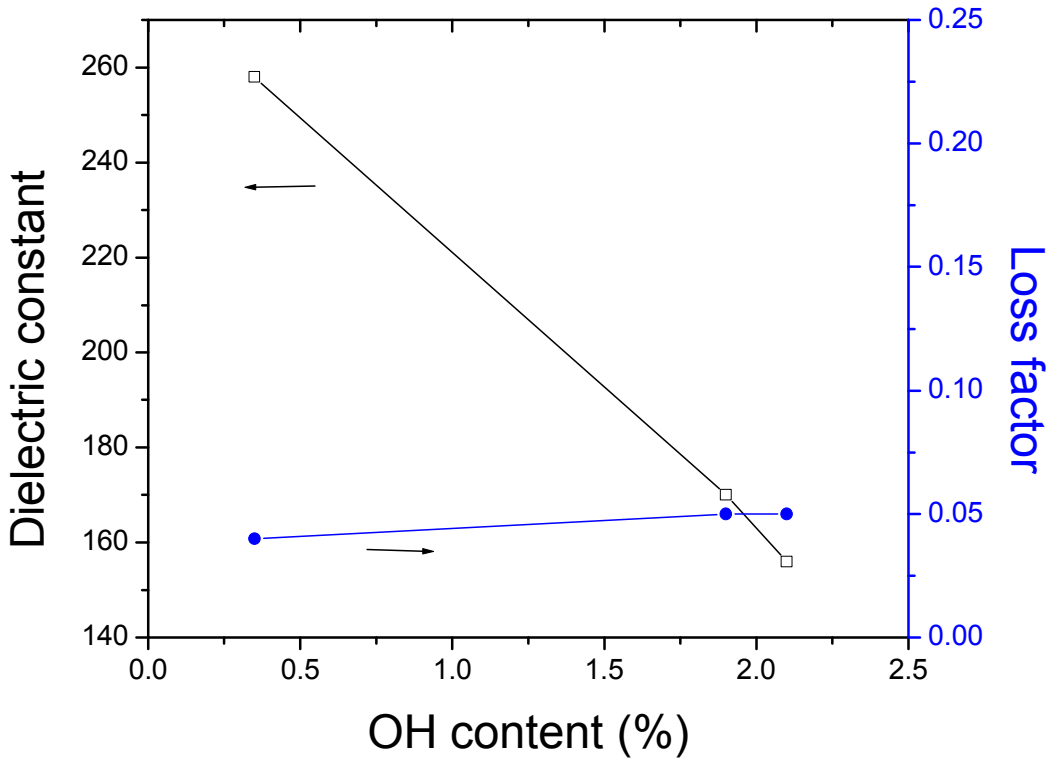

Fig. 21b. Dielectric properties of barium titanate aged in basic water with increasing OH content

The summary of the results is tabulated in Table 4.

Table 4. Variations in OH content, dielectric constant and dielectric loss values with respect to different pH treatments of barium titanate powder.

BT treatments	Calcined temperature	Lattice OH %	Dielectric constant (K)	Loss factor	% increase in K of NMP treated powder (291)
Acidic water	25	0.67	162	0.05	44
	200	0.58	180	0.04	38
	1100	0.15	273	0.03	6
Basic water	25	2.1	156	0.05	46
	200	1.9	170	0.05	41
	1100	0.35	258	0.04	11

Conclusions

Barium titanate treated with NMP contains a lower concentration of lattice hydroxyl group, resulting in a small lattice strain. The tetragonality in the hydrothermal barium titanate particles is restored by a one-step chemical treatment. The lattice hydroxyls in barium titanate were effectively extracted by the NMP treatment. As hypothesized, the lattice hydroxyl release is the reason of the tetragonality recovery. This method can be considered as a complementary treatment to promote the phase transition of cubic barium titanate and to synthesize tetragonal ferroelectric nanoparticles.

XRD confirms the tetragonality with the peak split at 45º and c/a ratio is obtained as 1.0078. FTIR investigations of hydrothermal barium titanate particles revealed a spectrum with a broad OH band in the wave number range of 2600 - 3600 cm^{-1}, indicating the presence of a significant concentration of surface OH groups in the film. A sharply-defined peak at 2931 cm^{-1}, attributed to lattice OH species, was also found. The apparent amount of lattice OH content was reported to be 0.35% for barium titanate powder treated with NMP at 200ºC for 24 hr. The simulation experiment adds value to the above statement as barium titanate calcined at 1100ºC in both acidic and basic waters show similar values which clearly indicates that elimination of OH initiates the tetragonality in a cubic barium titanate. Dielectric studies provide strong evidence to the hypothesis made as the dielectric constant of NMP treated barium titanate powder particle is 291, 64% higher than the value of as-received barium titanate, 177 and the loss factor was observed to constant at 0.03. Hence, extraction of hydroxyl ions, in particular the lattice OH, increases the dielectric constant of the powder.

REFERENCES

1. D. C. Dube and S. J. Jang, Proc. Symp. Ceram. Dielectr. 8 (1985) 315.

2. D. Pozar, Microwave Engg. (Addison-Wesley, Massachusetts, 1990) 313.

3. S. K. Bhattacharya and R. R. Tummala, *J. Mater. Sci. Mater. Electron.* 11 (2000) 253.

4. Y. Rao, S. Ogitani, P. Kohl and C. P. Wong, Proc. Elec. Components and Technology. (2000) 183.

5. B. A. Schutzberg, C. Huang, S. Ramesh and E. P. Giannelis, Proc. Elec. Components and Technology. (2000) 1564.

6. S. Ogitani, S. A. Bidstrup-Allen and P. A. Kohl, IEEE Trans. Advanced Packaging 23 (2000) 313.

7. S. D. Cho, S. Y. Lee, J. G. Hyun and K. W. Paik, Mat. Sci. Eng. B110 (2004) 233.

8. S. D. Cho, S. Y. Lee, J. G. Hyun and K. W. Paik, Mat. Sci: Elec. 16 (2005) 77.

9. N. G. Devaraju, B. I. Lee, E. S. Kim, Microelec. Engg. 82 (2005) 71.

10. T. Yamada, T. Ueda and T. Kitayama, J. Appl. Phys. 53 (1982) 4328.

11. N. Jayasundere and B. V. Smith, ibid. 73 (1993) 2462.

12. K. Mazur, *Plast. Eng.* 28 (1995) 539.

13. J. C. Maxwell-Garnett, Philos. Trans. R. Soc. London Ser. A, 203 (1904) 385.

14. D. K. Dasgupta and K. Doughty, Thin Solid Films, 158 (1988) 93.

15. D. Stauffer, A. Aharony, Introduction to percolation theory. Taylor & Francis, 1991.

16. M. Sahimi, Application of percolation theory. Taylor & Francis, 1994.

17. B. Sareni, L. Krahenbuhl, and A. Beroual, J. Appl. Phys., 85 (1997) 2375.

18. G. W. Milton, J. Appl. Phys., 52 (1981) 5286.

19. R. Waser, Integr. Ferroelectr. 15 (1997) 39.

20. G. Arlt, D. Henning and G. De With, ibid. 58 (1985) 1619.

21. S. Wada, H. Yasuno, T. Hoshina, S-M. Nam, H. Kakemoto, T. Tsurumi, Jpn. J. Appl. Phys. 42 (2003) 6188.

22. Y. Rao, J. Qu, T. Marinis, IEEE Trans. Components and Packaging Tech., 23 (2000) 680.

23. G. Arlt, J. Mat. Sci. 25 (1990) 2655.

24. D. H. Kuo, C. C. Chang, T. Y. Su, W. K. Wang and B.Y. Lin, Mat. Chem. & Phy. 85 (2004) 201.

25. D. Sinha and P. K. C. Pillai, J. Mat. Sci. Lett., 8 (1989) 673.

26. B. I. Lee, X. Wang, S. J. Kwon, H. Maie, R. Kota, J. H. Hwang, J.G. Park, M. Hu., Microelec. Engg. 83 (2006) 463.

27. Y. Rao, C. P. Wong, J. Qu, IEEE Trans. Electronic Components & Tech. Conference, (2000) 615.

28. S. K.Bhattacharya, P. M. Raj, D. Balaraman, H. Windlass, R. R. Tummala, Circuit World, 30/1 (2003) 31.

29. R. N. Das, M. D. Poliks, J. M. Lauffer, V. R. Markovich, "High Capacitance, Large Area, Thin Film, Nanocomposite Based Embedded Capacitors"

30. W. Hitesh, R. P. Markondeya, D. Balaraman, S. K. Bhattacharya, R. Tummala, IEEE Trans. Electron. Pack. Man. 26 (2003) 2.

31. Y. Rao, A. Takahashi, C. P. Wong, Composites: A 34 (2003) 1113

32. J. Andresakis, T. Yamamoto, N. Biunno, Circuit World 30/1 (2003) 36

33. S. Ogitani, A. S. Bidstrup, P. Kohl, IPC conf., San Diego, (2000)

34. S. D. Cho, J. Y. Lee, K. W. Paik, Electron. Compon. Technol. Conference (2002) 504

35. N. Manish, A. C. Jeanine, S. Lawrence Jr., A. Sen., Chem.Mater. 3 (1991) 201

36. N. Halder, S. A. Das, S. K. Khan, A. Sen, H. S. Maiti, Mater. Res. Bull. 34 (1999) 545

37. R. Chen, X. Wang, Z. Gui, L. Ti, J.Am. Ceram. Soc, 86 (2003) 1022
38. C. Pecharroman, J. S. Moya, Adv. Mater. 12 (2000) 294

39. C. W. Nan, Prog. Mater. Sci. 37 (1993) 1

40. C. W. Nan, Phys. Rev. B 63 (2001) 176201

41. D. A. G. Bruggeman, Ann. Phys. (Leipzig) 24 (1935) 636

42. N. Jayasundere, B.V. Smith, J. Apl. Phy. 34 (1995) 6149

43. C. Pecharroman, B. F. Esteban, J. S. Moya, Adv. Mater. 13 (2001) 1541

44. J. J. Wu, D. S. McLachlan, Phys. Rev. B 56 (1997) 1236

45. J. J. Wu, D. S. McLachlan, Phys. Rev. B 58 (1998) 14880

46. C. Brosseau, J. Appl. Phys. 91 (2002) 3197

47. Y. Rao, C. P. Wong, IEEE Proc. Electron. Compon. Technol. Conf. (2002) 920

48. Z. M. Dang, Y. H. Lin, C. W. Nan, Adv. Mater. 15 (2003) 1625

49. Z. M. Dang, Y. Shen, C. W. Nan, Appl. Phys. Lett. 81(2002) 4814

50. D. Stauffer, Phys. Reports 54 (1979) 1

51. N. R. Jana and X. G. Peng, J. Am. Chem. Soc. 125 (2003) 14280

52. S. H. Chen, K. Kimura, Langmuir 15 (1999) 1075-1082.

53. B. I. Lee, X. Wang, S. J. Kwon, H. Maie, R. Kota, J. H. Hwang, J. G. Park, M. Hu., Microelectron. Eng. 83 (2006) 463.

54. R. Kota, A. F. Ali, B. I. Lee, M. M. Sychov, Microelectron. Eng. (submitted)

55. Lai Qi, Synthesis and dielectric properties of ceramic-metal-polymer nano composites

56. S. Li, J. A. Eastman, Z. Li, C.M. Foster, R. E. Newnham, L. E. Cross, Phys. Lett. A (1996) 212, 341.

57. C. L. Wang, S. R.P. Smith, J. Phys.: Condens. Matter. 7 (1995) 7163.

58. B. Jiang, L. A. Bursill, Phys. Rev. B 60 (1999) 9978.

59. W. L. Zhong, Y. G. Wang, P. L. Zhang , B. D. Qu, Phys. Rev. B 50 (1994) 698.
60. H. Huang, C. Q. Sun, P. Hing, J. Phys.: Condens. Matter. 12 (2000) L127.

61. M. A. Pena, J. L. G. Fierro, Chem. Rev. 101 (2001) 1981.

62. A. S. Bhella, R. Guo, R. Roy, Mater. Res. Innovations, 4 (2000) 3.

63. P. K. Dutta, R. Asiaie, S. K. Akbar, W. Zhu, Chem. Mater. 6 (1994) 1542.

64. P. Duran, D. Gutierrez, J. Tartaj, C. Moure, Ceram. Int. 28 (2002) 283.

65. P. R. Arya, P. Jha, A. K. Ganguli, J. Mater. Chem.13 (2003) 415.

66. S. Bhattacharya, R. Tummalla, J. Mater. Sci. Mater. Electronics 11 (2000) 253.

67. D. H. Yoon, B. I. Lee, J. Ceram. Process. Res. 3 (2002) 41.

68. C. D. Chandler, C. Roger, M. H. Smith, J. Chem. Rev. 93 (1993) 1205.

69. D. Henning, M. Klee, W. Waser, Adv. Mater. 3 (1991) 334.

70. G. Arlt, D. Hennings, G. de With, J. Appl. Phys. 58 (1985) 1619.

71. I. J. Clark, T. Takeuchi, N. Ohtori, D. C. Sinclair, J. Mater. Chem. 9 (1999) 83.

72. S. Schlag, H. F. Eicke, Solid State Commun. 91 (1994) 883.

73. K. Ishikawa, K. Yoshikawa, N. Okada, Phys. Rev. B 37 (1988) 5852.

74. Y. Kobayashi, A Nishikata, T. Tanase, M. Konno, J. Sol-Gel Sci. Technol. 29 (2004) 49.

75. T. Takeuchi, M. Tabuchi, K. Ado, K. Honjo, O. Nakamura, H. Kageyama, Y. Suyama, N. Ohtori, M. Nagasawa, J. Mater. Sci. 32 (1997) 4053.

76. L. Qi, B.I. Lee, P. Badheka, D. H. Yoon, W. D. Samuels, G. J. Exarhos, J. Eur. Ceram. Soc. 24 (2004) 3553.
77. L. Qi, B. I. Lee, P. Badheka, L.Q Wang, P Gilmour, W. D. Samuels, G. J. Exarhos, Mater. Lett. 59 (2005) 2794.

78. D. Hennings and S. Shreinmacher, J. Eur. Ceram. Soc. 9 (1992) 41.

79. S. Wada, T. Suzuki, and T. Noma, J. Ceram. Soc. Jpn. 103 (1995) 1220.

80. T. Noma, S. Wada, M. Yano, and T. Suzuki, J. Appl. Phys. 80 (1996) 5223.

81. D. F. K. Hennings, C. Metzmacher, and B.S. Schreinemacher, J. Am. Ceram. Soc. 84 (2001) 179.

82. A.T. Chien, L. Zhao, M. Colic, J.S. Speck, and F.F. Lange, J. Mater. Res. 14 (1999) 3330.

83. V. M. Fuenzalida, M. E. Pilleux, and I. Eisele, Vacuum 55 (1999) 81.

84. S. Wada, T. Suzuki, T. Noma, J. Ceram. Soc. Jpn. 104 (1996) 383.

85. T. Yamamoto, H. Niori, H. Moriwake, Jpn. J. Appl. Phys. 39 (2000) 5683.

86. E. Ciftci, M. N. Rahaman, J. Mater. Sci. 36 (2001) 4875.

87. P. Badheka, L. Qi, B. I. Lee, J. Eur. Ceram. Soc. 26 (2006) 1393

88. S. K. Patil, N. Shah, F.D. Blum, M.N. Rahaman, J. Mater. Res. 12 (2005) 3312.

89. B. I. Lee, J. Electroceramics , 3 (1999) 51

90. S. Lu, B. I. Lee, Mann, L., Mater. Lett., 43 (2000) 102

91. S. Lu, B. I. Lee, Mater. Res. Bull., 35 (2000) 1303

92. M. H. Frey, D. A. Payne, Phys. Rev., B 54 (1996) 3158